The Pennsylvania State University

The Graduate School

College of Engineering

MODELING AND CONTROL OF AN AUXILIARY POWER UNIT FOR A PLUG-IN HYBRID ELECTRIC VEHICLE

A Thesis in

Electrical Engineering

by

Yichong Yu

© 2014 Yichong Yu

Submitted in Partial Fulfillment
of the Requirements
for the Degree of

Master of Science

August 2014

The thesis of Yichong Yu was reviewed and approved* by the following:

Jeffrey Mayer
Associate Professor of Electrical Engineering
Thesis Advisor

Minghui Zhu
Assistant Professor of Electrical Engineering

Kultegin Aydin
Professor of Electrical Engineering
Head of the Department of Electrical Engineering

*Signatures are on file in the Graduate School

ABSTRACT

With increasing petroleum price and fuel economy standards, cleaner and sustainable energy solutions have been demanded in vehicle industry. Plug-in hybrid electric vehicles, which are powered by an internal combustion engine and an electric motor with a battery pack, have the ability of achieving superior fuel economy. The hybridization and electrification of the powertrain requires an effective and optimized model and control system. On the other hand, modeling and simulation tools have been developing very fast. The simulation tools have become very important when complex system model based control design is applied. The modeling and simulation tools are able to design the whole process and control strategy, rather than just being used to validate or test the real data.

The study in this thesis was based on the EcoCAR 2 competition. The objective of the competition is to reduce fuel consumption, reduce well-to-wheel greenhouse gas emissions, reduce criteria tailpipe emissions and maintain consumer acceptability in the areas of performance, utility, and safety. This thesis will present the methodology for modeling the Auxiliary Power Unit (APU) and control strategy design and optimization. The engine and generator models will form the APU model. Several interpolation methods are used to refine energy and fuel efficiency. Software-in-the-loop (SIL) simulation is used to optimize the control strategy. Finally, the experiment result demonstrates the performance improvements.

TABLE OF CONTENTS

List of Figures v

List of Tables vi

Acknowledgements vii

Chapter 1 Introduction 1

1.1 Background 2
1.1.1 Motivation 2
1.1.2 Plug-in Hybrid Electric Vehicle Architectures 5
1.1.3 EcoCAR 2 Competition and Penn State Advanced Vehicle Team 8
1.2 Contribution 12
1.3 Outline 12

Chapter 2 Auxiliary Power Unit Specifications 14

2.1 Internal Combust Engine 15
2.2 Generator 17
2.3 Vehicle Interface 20
2.3.1 Energy Storage System 20
2.3.2 Master Vehicle Controller 21

Chapter 3 Auxiliary Power Unit Model 23

3.1 Engine Model 25
3.1.1 Torque Map 26
3.1.2 Brake Specific Fuel Consumption Map 30
3.2 Generator Model 32
3.2.1 Torque Block 33
3.2.2 Generator Power Losses Map 34
3.3 Generator Speed Control Block 40

Chapter 4 Auxiliary Power Unit Control 43

4.1 Introduction 43
4.2 APU Mode and Operation Determination 45
4.2.1 APU Mode Calculation 45
4.2.2 Set Point Calculation 47
4.3 Engine Control 49

Chapter 5 Auxiliary Power Unit Performance 51

5.1 Simulation of the Auxiliary Power Unit 51
5.1.1 Simulation of APU Model 51
5.1.2 Simulation of APU Mode Calculation 63
5.1.3 Simulation of Set Points Calculation 65

5.1.4 Simulation of Engine Control 69
5.2 Experiment of the Auxiliary Power Unit 71
5.2.1 Equipment Used 71
5.2.2 Measurement 71
5.2.3 Results 73

Chapter 6 Summary and Conclusions 75

6.1 Summary 75
6.2 Future work 76

Appendix Vehicle Model 77

References 78

LIST OF FIGURES

Figure 1-1. U.S. Vehicle Fleet Daily Gasoline Consumption 3

Figure 1-2. Global Daily Petroleum Consumption 3

Figure 1-3. Global Fossil Carbon Emissions 4

Figure 1-4. Schematic diagram of parallel architecture for a P/HEV 7

Figure 1-5. Schematic diagram of series PHEVs architecture 8

Figure 1-6. V-Diagram [9] 10

Figure 1-7. Penn State's EcoCAR 2 vehicle architecture 11

Figure 2-1. Exploded view of APU assembly 14

Figure 2-2. Block diagram of the generator 17

Figure 2-3. Contour plot of generating efficiency map from user manual [11] 20

Figure 2-4. The relationship between the APU, the ETS and the ESS 21

Figure 3-1. APU model 24

Figure 3-2. The flow chart of APU model 24

Figure 3-3. Engine model 26

Figure 3-4. Dynamometer platform 27

Figure 3-5. Comparison of original engine map and three expended engine maps 30

Figure 3-6. Energy and energy consumption calculation block 31

Figure 3-7. Plot of Weber MPE 750 BSFC map. 31

Figure 3-8. Generator model 32

Figure 3-9. Generator torque calculation block 33

Figure 3-10. Delaunay triangulation plot of efficiency Map 35

Figure 3-11. Contour plot of generating efficiency map from data table 35

Figure 3-12. Contour plot of generating Efficiency Map 36

Figure 3-13. Contour plot of three expended efficiency data map 39

Figure 3-14. Comparison of the original and the expended efficiency data maps 40

Figure 3-15. Generator speed control function block 41

Figure 4-1. APU controller block diagram 44

Figure 4-2. State flow of APU mode calculation 46

Figure 4-3. APU set points calculation 47

Figure 4-4. The limitation of engine temperature and battery temperature 48

Figure 4-5. State flow of engine operation 50

Figure 5-1. Comparison of reference generator speed and simulated generator speed when the Run 4 used 52

Figure 5-2. Comparison of reference output power of generator and simulated output power of generator when the Run 4 used 53

Figure 5-3. Comparison of reference generator speed and simulated generator speed when the Run 9 used 53

Figure 5-4. Comparison of reference output power of generator and simulated output power of generator when the Run 9 used 54

Figure 5-5. Throttle-speed-APU power map 55

Figure 5-6. Plot of throttle-speed-consumption map 56

Figure 5-7. The aerial views of throttle-speed-power map (Left) and throttle-speed-consumption map (Right) 56

Figure 5-8. Vibration of engine speed at 3000 RPM 57

Figure 5-9. The inertia torque (Left) and torque resulting from gas pressure (Right) [14] 58

Figure 5-10. The total torque on the crankshaft for a single cylinder engine [14] 58

Figure 5-11. The throttle control loop 59

Figure 5-12. The spectra of speed vibration and current vibration at speed 3000rpm 60

Figure 5-13. The spectra of speed vibration and current vibration at speed 3500rpm 60

Figure 5-14. The spectra of speed vibration and current vibration at speed 4500rpm 61

Figure 5-15. Simulation layout of APU mode calculation block 63

Figure 5-16. Results of the battery power calculation model simulation 64

Figure 5-17. Simulation layout of APU set points calculation block 66

Figure 5-18. Results of the set points calculation block simulation with abnormal temperature 67

Figure 5-19. Results of the set points calculation block simulation with normal temperature 68

Figure 5-20. Simulation layout of engine control block 69

Figure 5-21. Results of the engine control block simulation 70

Figure 5-22. Measurement of APU model 72

Figure 5-23. Measurement of APU control algorithm 73

LIST OF TABLES

Table 1-1. List of HEV development to date [4] 5

Table 1-2. Emissions and fuel cost comparison 8

Table 1-3. The List of key subsystems and components 11

Table 2-1. APU component technical specifications 15

Table 3-1. Engine map from dynamometer 27

Table 3-2. The tuned engine map 28

Table 3-3. Continuous torque map and peak torque map 33

Table 3-4. Efficiency data table 36

Table 4-1. APU mode in each state 46

Table 4-2. Set points information 48

Table 5-1. Speed and throttle information of simulation datasets 52

Table 5-2. Error between the reference data and the simulation results 54

Table 5-3. Throttle-speed-consumption map 55

Table 5-4. The output power and fuel consumption of three set points 56

Table 5-5. The relationship among mean speed of engine, the engine fire frequency and the inertia frequency 61

Table 5-6. The alias frequency 62

Table 5-7. The inputs of the APU mode calculation block simulation 63

Table 5-8. The relationship among charge sustaining switch, engine switch and APU mode 64

Table 5-9. The inputs of the set points calculation block simulation with abnormal temperature 67

Table 5-10. The inputs of the set points calculation block simulation with normal temperature 68

Table 5-11. The inputs of the engine control block simulation 70

Table 5-12. Result of point-by-point measurement 72

Table 5-13. Result of point-by-point measurement and result of APU model simulation 73

ACKNOWLEDGEMENTS

I would like to acknowledge and express my sincere gratitude to my advisor, Professor Jeffrey Mayer for his continuous support of my study and research, for his guidance, patience, immense knowledge and providing me with an excellent atmosphere for doing research.

I would also like to express my thanks to the Advanced Vehicle Team of Penn State. It was a pleasure to work in the AVT. I would like to thank the team members, Chris Golecki, Chris Monaco, Ken Swidwa and Jim Kreibick for their knowledge, assistance and support of my study.

Finally, my appreciation goes to my wife and parents. No words can express my appreciation for their unconditional support and inspiration. I will continue to study and work hard so that their love and support is deserved.

Chapter 1

Introduction

The study in this thesis is based on the Penn State Advanced Vehicle Team's entry in the EcoCAR 2: Plugging Into the Future competition. This three years competition (July 2011 to June 2014) is sponsored by the U.S. Department of Energy (DOE) and General Motors (GM) and is organized by Argonne National Laboratory. There are 15 teams from North American universities. The goal is to design and build a Plug-in Hybrid Vehicle (PHEV) using a 2013 Chevrolet Malibu as a base vehicle and applying a simplified version of GM's global vehicle development process. The focus of the third year of the competition, the period during which the work reported here was performed, was refining the vehicle to achieve a "99% Buyoff" vehicle; that is, a vehicle that would have 99% consumer acceptability in terms of performance, utility, and safety.

A hybrid electric vehicle is a type of hybrid vehicle and electric vehicle which combines a conventional internal combustion engine propulsion system with an electric propulsion system [1]. A PHEV is an HEV that utilizes rechargeable batteries, or another energy storage device, that can be restored to full charge by connecting a plug to an external electric power source. A PHEV shares the characteristics of both a hybrid electric vehicle and an all-electric vehicle [1].

The auxiliary power unit (APU) is an important component of a PHEV. It provides a second source of energy for the PHEV, allowing for significantly greater range than an all-electric vehicle.

The interrelated goals of this study are to tune an APU model and to improve the performance of the APU and overall vehicle through increased attention to the APU control algorithm. The APU model was originally developed in Year 1. The APU control algorithm was originally developed in Year 1 and tested in both simulation and vehicle platforms in Year 2.

1.1 Background

1.1.1 Motivation

In the US and around the world, we are experiencing an upward trend in gasoline consumption. Figures 1-1 and 1-2 are based on data are from U.S. Energy Information Administration annual report [2] and show that in 1980 approximately 273 million gallons of gasoline were consumed per day by vehicles in the US, and approximately 45 million barrels of petroleum were consumed per day globally. Consumption increased significantly between 1980 and 2011 to the point that over 395 million gallons of gasoline and 3.2 billion gallons of petroleum were consumed per day in the U.S. and globally, respectively.

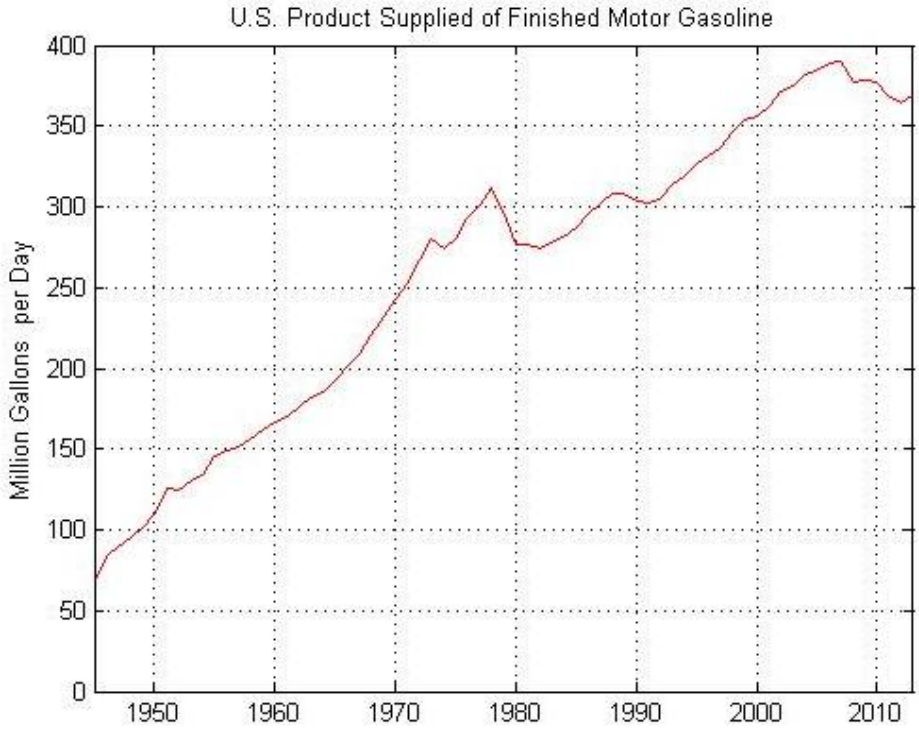

Figure 1-1. U.S. Vehicle Fleet Daily Gasoline Consumption

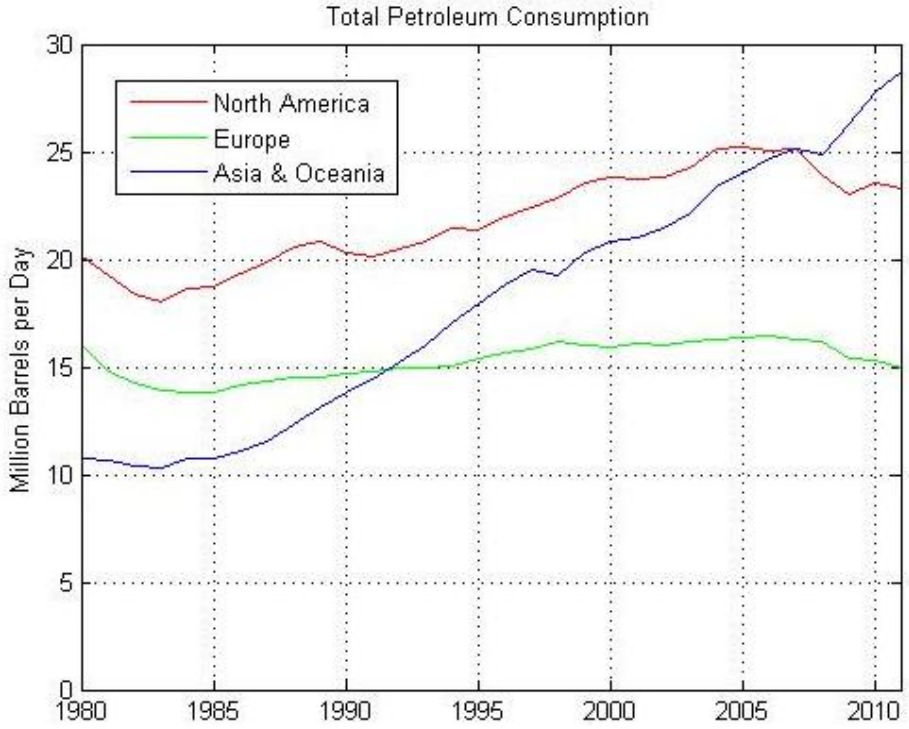

Figure 1-2. Global Daily Petroleum Consumption

At the same time, greenhouse gas emissions have grown significantly as well. Figure 1-3 shows that in 2009 about 17.4 billion tons of carbon were released into the atmosphere because of the petroleum consumption [3]. Although vehicles are not the only consumers of petroleum or sources of carbon emission, they are a major one.

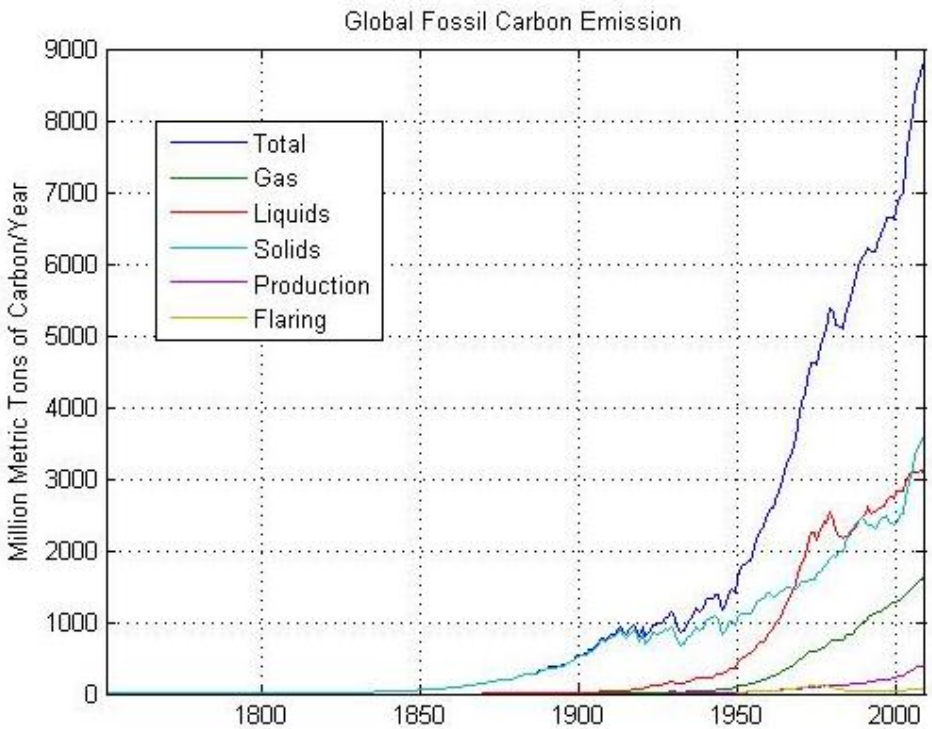

Figure 1-3. Global Fossil Carbon Emissions

Due to pressing environmental concerns and demands to decrease energy use, many auto makers began to develop Hybrid Electric Vehicles (HEV) as a next generation vehicle (Table 1-1).

Manufacturers and Vehicles		Year	Type
Toyota	Prius, Camry, Highlander	1997	Sedan, SUV
Lexus	RX400h, LS600H	2005	Sedan, SUV
Honda	Insight, Civic, Accord	2005	Sedan, SUV
GM	Silverado, Saturn, Equinox, Tahoe, Yukon	2007	Truck, SUV
GM	New Flyer	2004	Heavy Bus
Chrysler	Durango, Ram	2005	Truck
Mercedes	Benz S	2006	Sedan
Ford	Escape, Mariner	2005	SUV
Hyundai, Renault, IVECO		2004	Various

Table 1-2. List of HEV development to date [4]

It is interesting to note that while HEV and PHEV technology has been developing very fast in the past few years, this technology has been around over 100 years. The Lohner-Porsche Elektromobile, which was one of the first hybrid cars in the world, appeared at the Paris Exposition of 1900 [5]. In 1905, an American engineer named H. Piper filed a patent for a petrol-electric hybrid vehicle that used an electric motor to assist an internal-combustion engine and could achieve 25 mph [5]. Nonetheless, the conventional engine still dominated the car industry for about 60 years, until the price of gasoline soared because of the Arab oil embargo of 1973. The U.S. congress passed the Electric and Hybrid Vehicle Research, Development & Demonstration Act of 1976 [5]. This legislation created new interest in electric vehicles. In 1997, Toyota introduced the first ICE based HEV to the Japanese market, the Toyota Prius. This was the first hybrid four-door sedan and it was available in the U.S. in 2000 [5].

1.1.2 Plug-in Hybrid Electric Vehicle Architectures

A hybrid electric vehicle (HEV) combines a conventional internal combustion engine (ICE) propulsion system with an electric propulsion system [1]. Thus, an HEV

permits the use of two different forms of energy. The first form is typically gasoline, but can also be diesel fuel, natural gas, or a biofuel. For any of these fuels, the energy is extracted via combustion, which is an irreversible process. The second form is electric energy stored in a battery pack, although other storage technologies such as ultra-capacitors and flywheels are possible. For any of these storage technologies, energy can flow bidirectionally. The advantage of a hybrid system is:

- Higher efficiency:
  - Electric propulsion system efficiency is higher than ICE propulsion system efficiency.
  - Electric propulsion system can recover, at least partially, vehicle kinetic energy during breaking as they permit reversible flow of energy.
- Better torque characteristics: electric machine has high torque at low speed, while ICE has low torque at low speed.
- Lower tail-pile emissions and fuel consumption: the electric machine has no tail-pipe emissions. In addition, the ICE can be shut down during breaking/stops, thereby reducing fuel consumption, as well as tail-pipe emissions.
- Smaller engine is possible: the ICE only needs to accommodate average load rather than peak load, thus a smaller, lighter engine is possible.

A Plug-in HEV (PHEV) has an internal combustion engine and an electric motor with a high capacity battery pack. A PHEV has the characteristic of both an HEV and an EV, and has the advantage of both an HEV and an EV as well:

- A PHEV has all the capabilities of a HEV but has lower fuel consumption and tail-pipe emissions, because a PHEV can be operated as an EV.

- An EV has driving range limited by the capacity of the battery pack, while a PHEV has a fuel tank and an ICE, and therefore the driving range of a PHEV is theoretically unlimited per periodic refilling the fuel tank.

There are two general classes of P/HEV architectures: parallel and series. A parallel architecture provides power to the wheels from both the ICE and an electric machine(s) [6], as illustrated in Figure 1-4. Because both the ICE and electric machine(s) can provide torque to the wheels, both of the engine and the motors can be downsized, making the parallel architecture more viable with lower costs and higher efficiency [4]. The major disadvantage of a parallel architecture is that the engine cannot be regulated to remain at its most effeiencent operating point because it is mechanically coupled to the wheels [7].

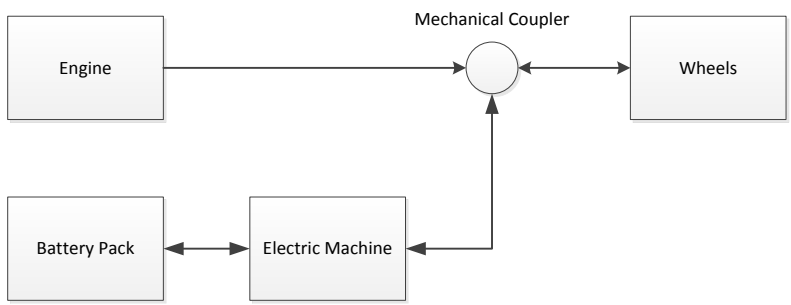

Figure 1-4. Schematic diagram of parallel architecture for a P/HEV

The series hybrid also employs an ICE, although it provides no power to the wheels. Instead, the ICE functions solely as prime mover for a generator, providing energy to charge the batteries. The wheels are powered solely by an electric motor(s), using the energy stored in the batteries [6]. The architecture is illustrated in Figure 1-5. It allows the engine run in its high efficiency speed and torque region. The main disadvantage is that mechanical power from the engine changes its form twice, from mechanical to electrical in the electric generator and from electrical to mechanical again in the electric motor [7], which will cause some power losses.

Figure 1-5. Schematic diagram of series PHEVs architecture

The battery pack can be charged either by connecting a plug to an external electric power source, or using an auxiliary power unit (engine and generator) to generate electric power. Table 1-2 shows that PHEVs have the significant ability to reduce fuel consumption and greenhouse gas emissions. A PHEV can play an important role in reducing petroleum consumption and greenhouse gas emission.

Emissions and Fuel Cost for a 100-Mile Trip		
Vehicle (compact sedans)	**Greenhouse Gas Emissions (pounds of CO2 equivalent)**	**Total Fuel Cost (Gallons)**
Conventional	87 lb CO_2	3.62
Hybrid Electric	57 lb CO_2	2.38
Plug-in Hybrid Electric	62 lb CO_2	1.92
All-Electric	54 lb CO_2	1.01

Source: US department of energy, http://www.afdc.energy.gov/vehicles/electric_emissions.php

Table 1-2. Emissions and fuel cost comparison

1.1.3 EcoCAR 2 Competition and Penn State Advanced Vehicle Team

EcoCAR 2: Plugging In to the Future is a three-year collegiate engineering competition sponsored by the U.S. Department of Energy and General Motors. It is organized by Argonne National Laboratory and there are 15 teams from North American universities. The technical goals are to design and integrate vehicle powertrains that, when compared to the production gasoline vehicle achieve the following: [8]

- Reduce fuel consumption
- Reduce well-to-wheel greenhouse gas emissions

- Reduce criteria tailpipe emissions
- Maintain consumer acceptability in the areas of performance, utility, and safety

General Motors provided each of the 15 teams with a 2013 Chevrolet Malibu to use as a base vehicle. The competition takes place over three years from 2011 to 2014. The focus of the competition is different each year reflecting the stages of General Motors global vehicle development process:

- First Year: Modeling and Simulation.
- Second Year: Implementing designs developed during the first year and integrating components into the vehicle to create a vehicle at the 65% buy-off point.
- Third Year: Vehicle refinement, expanding on the efforts of years past by enhancing designs from the first two years. The final product is a highly-refined automobile at the 99% consumer buy-off point.

The General Motors global vehicle development process is an extensive set of design, modeling, simulation and validation. The vehicle development process (VDP) serves as a roadmap for the engineering process of designing, building and refining their advanced technology vehicles. Following a VDP will give the teams an opportunity to improve their vehicles efficiency while retaining consumer acceptability, performance and safety [8].

The PSU AVT's development process followed the V-Diagram, as shown in Figure 1-6. The process has two parts: verification and validation. The development process begins by defining the control system requirements and the final stage of verification is the software implementation. With the completion of the software

implementation, the validation stage of development begins. The first stage is unit testing and the last step is validating control system in vehicle.

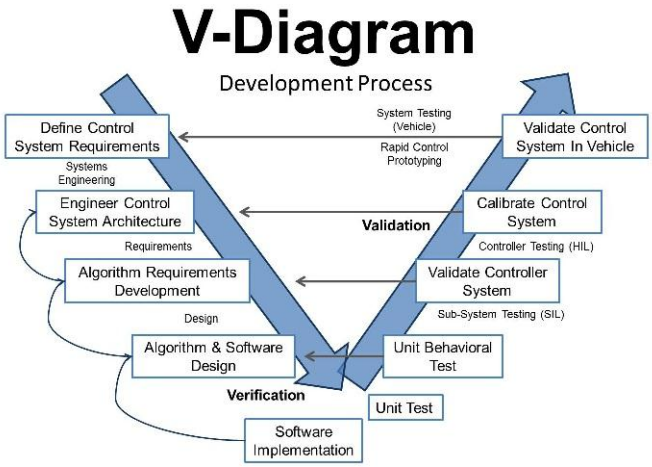

Figure 1-6. V-Diagram [9]

The Pennsylvania State University Advanced Vehicle Team (PSU AVT) has participated in eight similar Department of Energy/Argonne National Laboratory vehicle competitions dating back to 1989. The previous competitions, however, were structured with a greater emphasis on the final product than on the design process. Consequently, the PSU AVT enjoys extensive corporate knowledge and experience in physical design, fabrication, and integration of vehicle subsystems but a more limited background in modeling, simulation, and control.

During the first year of the EcoCAR 2competition, the PSU AVT elected to use the series PHEV architecture shown in Figure 1-7 with the components listed in Table 1-3. The Team also created a Vehicle Technical Specifications, developed basic control code, and implemented required Software-in-the-Loop (SIL) and Hardware-in-the-Loop (HIL) simulations

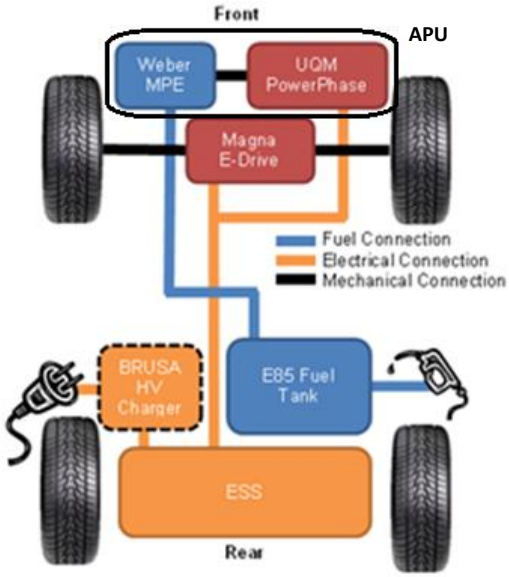

Figure 1-7. Penn State's EcoCAR 2 vehicle architecture

Divetrain	Auxiliary Power Unit (APU)
Magna E-Drive	Weber MPE 750
	UQM PowerPhase 75
Energy Storage System(ESS)	**Master Vehicle Controller**
Six A123 15s3p Modules	Motohawk ECM-5554-112-0904
A123 Battery Control Module (BCM)	
A123 Current Shunt Module (CSM)	
A123 Electrical Distribution Module (EDM)	

Table 1-3. The List of key subsystems and components

In the second year of the competition, the AVT focused on fabrication and integration of subsystem components and on developing the supervisory control algorithm through both simulation and in-vehicle testing.

The final product of the second year is a functional vehicle that provides a stable test platform to refine into a fully production ready vehicle in the third year [9].

In the third year of the competition, the AVT focused on vehicle refinement, expanding on the efforts of years past by enhancing designs form the first two years. The goal of Year 3 is accomplished by increasing consumer appeal and refining the mechanical, electrical, and control systems. Mechanical refinements include aerodynamic

improvements and light weighting. Electrical refinements focused on increasing the electrical system reliability. Controls system refinements include calibration from testing, parameter optimization, reliability improvements, and the addition of consumer-friendly features. [9]

1.2 Contribution

The main contribution of this thesis is the development of the APU model and APU control strategy. The contribution can be summarized as follows:

- Refined APU model by improving engine torque map, generator efficiency map, and fuel consumption map.
- Validated APU model using measurement data.
- Refined APU control algorithm.
- Analyzed measured oscillations in engine speed and throttle position. The result can be used for future research on engine control.

1.3 Outline

This chapter provided an overview of PHEV technology, Penn State's involvement in the EcoCAR 2 competition, and the contribution of this work to modeling and control of the Auxiliary Power Unit (APU) in the Penn State EcoCAR 2 vehicle.

In Chapter 2, specifications of the APU are described along with its vehicle interface.

In Chapter 3, modeling of the APU is explained. Several important data maps are analyzed and improved.

Chapter 4 elucidates the APU control strategy. The chapter also explains how the control algorithm is implemented in the model.

Experiment and validation are described in Chapter 5.

In Chapter 6, a summary is provided, and the future works are described.

Chapter 2

Auxiliary Power Unit Specifications

In a Plug-in Hybrid Electric Vehicle (PHEV) with a series architecture, the internal combusting engine and generator together are usually considered to be a vehicle subsystem called the Auxiliary Power Unit (APU), because this energy source is not required for operation of the vehicle but rather is used to supplement the energy storage system (battery pack).

The auxiliary power unit in the PSU EcoCAR 2 vehicle is implemented using a Weber MPE 750 engine and a UQM PowerPhase® 75 generator. The two are joined by a bell housing that contains a flywheel and rubber torsional coupling [9]. Figure 2-1 shows an assembly drawing of the APU, and Table 2-1 lists the high-level technical specifications of the APU components.

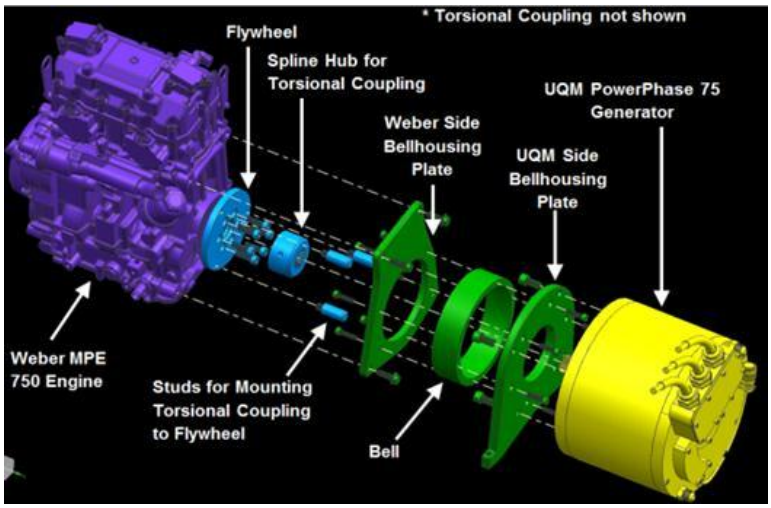

Figure 2-1. Exploded view of APU assembly

Weber MPE 750 naturally-aspirated 750cc engine (w/ automotive camshaft) specifications	
Max Power (kW)	40 @6500 RPM
Max Torque (N m)	67 @5000 RPM
Mass [dry] (kg)	48
UQM Technologies PowerPhase® 75 Traction System specifications (generator mode)	
Continuous Power (kW)	45
Peak Power (kW)	75
Mass [dry] (kg)	41

Table 2-1. APU component technical specifications

2.1 Internal Combust Engine

In an internal combustion engine (ICE), the combustion of a fuel and oxidizer occurs in a combustion chamber that is an integral part of the working fluid flow circuit. Expansion of the high-temperature and high-pressure combustion gases applies force directly to movable components of the engine, typically pistons or turbine blades. The force applied over the distance of the motion is mechanical work. Thus, the chemical energy of the fuel is transformed into mechanical energy.

For a reciprocating piston engine, the translational motion of the piston is converted to rotational motion via a connecting rod and crank. Thus, the mechanical energy is delivered as a torque acting over an angle. A piston is the central working part of a reciprocating engine, it travels in a cylinder. The combustion of the fuel and air in the cylinder results in a force on the crown of the piston. Each cycle of reciprocation consists of two opposite motions: there is a motion in one direction, and then a motion back in the opposite direction. Each of these is called a stroke [1]. The throttle is used to control the mass air flow, which in turn affects the output torque of the engine.

A Weber MPE 750 made by Weber Motor based in Markdorf, Germany is used as the APU engine for the PSU vehicle. It is two-cylinder, four-stroke engine that is naturally aspirated and has a 11.5:1 compression ratio. It is certified by the Environmental Protection Agency (EPA) for gasoline.

The Brake specific fuel consumption (BSFC) map is used to find the fuel energy and fuel consumption. BSFC is a measure of the fuel efficiency of a shaft reciprocating engine. It is the rate of fuel consumption divided by the power produced. It may also be thought of as power-specific fuel consumption, for this reason. BSFC allows the fuel efficiency of different reciprocating engines to be directly compared [1]. It can be expressed as

$$\mathrm{BSFC} = \frac{\text{fuel consumption rate } ({}^{g}/_{\mathrm{h}})}{\text{power produced (kW)}}$$

According to the Weber MPE 750 manual [10], the value of the best point of BSFC is 249 g/kWh when the engine speed is about 4000 rpm and the torque is 60 Nm.

In the project, the engine is fueled with E85 (85/15 % v/v ethanol/gasoline). E85 has 33% less energy content than 100% gasoline and 30% less than the E10 which is sold by almost all retailers in the US. [1] The fuel consumption rate of E85 is greater than that of E10 and the average ratios of fuel economy for E85 versus E10 are 1.3. Therefore, the BSFC of the engine when E85 is used can be represented as:

$$\mathrm{BSFC}_{\mathrm{E85}} = \frac{\text{fuel consumption rate } ({}^{g}/_{\mathrm{h}})}{\text{power produced (kW)}} \times 1.3$$

Then the value of best point of BSFC becomes 324 g/kWh.

2.2 Generator

A UQM PowerPhase® 75 made by UQM Technologies based in Colorado is used as the APU generator for the PSU vehicle. The PowerPhase® 75 is actually a system comprised of two components: (1) a 3-phase brushless permanent magnet machine that converts the mechanical energy from the engine into three-phase ac voltages and currents and (2) a controller that converts the 3-phase ac quantities to dc quantities required for the energy storage system. A block diagram of the generator system is shown Figure 2-2. The energy flows are bidirectional because the system is used as a motor when starting the engine. The PowerPhase® 75 has a peak power rating of 75 kW and a continuous power rating of 41 kW. The distinction between peak and continuous ratings arises due to the transient thermal characteristics of the liquid-cooled power inverter. The dc bus interface has an operating range of 250 V to 400 V and a current limit of 400 A.

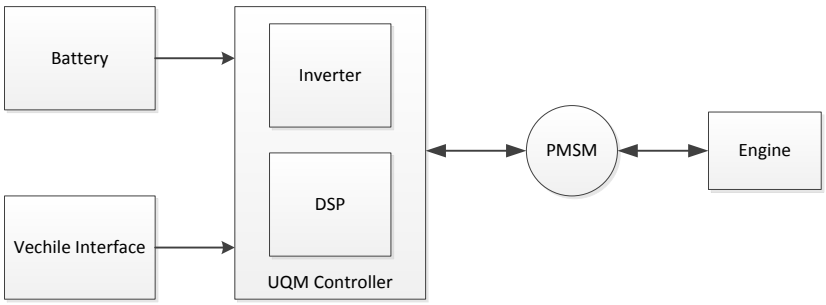

Figure 2-2. Block diagram of the generator

The vehicle interface for the generator system supports three methods for accepting control inputs. Each of these methods is associated with one or more of three control modes that are described subsequently. The three methods are:

- CAN[1] bus: commanded torque, speed, or voltage inputs are accepted via the CAN bus.

[1] CAN stands for Control Area Network, and CAN bus refers to an intra-vehicle digital communication system that is a de-facto standard in the automotive industry. Additional information about CAN bus is provided in Section 2.3.

- Analog input signal ports: commanded torque or speed inputs are accepted via two analog signal ports.
- System Configuration: set point values for torque or speed can be programmed.

The three control modes are:

- Torque control operational mode

When communicating via CAN bus, the commanded torque value is specified as the data word in a Universal Command.

When using analog torque control, commanded torque is represented as a percentage of full scale for the analog input signal ports. The “ACCEL” port is used for a positive torque, and “BRAKE” port is used for negative torque.

- Speed control operational mode

When communicating via CAN bus, the commanded speed value is specified as the data word in a Universal Command. A torque limit can also be specified in in the same way.

When using analog speed control, commanded speed is represented as a percentage of full scale for the “ACCEL” analog signal input port. A torque limit is represented as percentage of full-scale torque for the “BRAKE” port.

- Voltage control operational mode

When communicating via CAN bus, the commanded voltage value is specified as the data word in a Universal Command.

When using analog voltage control, the motor controller tries to maintain a requested voltage level. When in Generator Mode, the voltage is maintained to the desired voltage that is stored in the System Configuration.

Speed control via the CAN bus is used in this project. The vehicle controller sends a speed command value to the generator controller via CAN bus.

The power losses map provides the efficiency information of the generator system. The efficiency of the generator system η_{gen} is related to the mechanical power, current from the generator and the battery voltage.

$$\eta_{gen} = \frac{I_{gen} \times V_{battery}}{P_{mechanical}}$$

The efficiency map is a three dimensional table which is indexed by the generator torque and generator speed. Since the engine and generator are directly coupled, the generator speed and engine speed are equal at any time. With the inputs of generator torque and generator speed, the map can output the efficiency. The theoretical output power can be calculated by $P(kw) = \frac{Torque(Nm) \times Speed(rad/s)}{1000}$. Therefore, the actual APU power can be calculated by:

$$APU\ Power = \text{Theoretical power} \times (1 - Power\ Losses)$$

UQM Technologies provides the generating efficiency map (Figure 2-3) and the efficiency data table of the generator. The solid line in Figure 2-3 is the peak power limit and the dashed line is the continuous power limit.

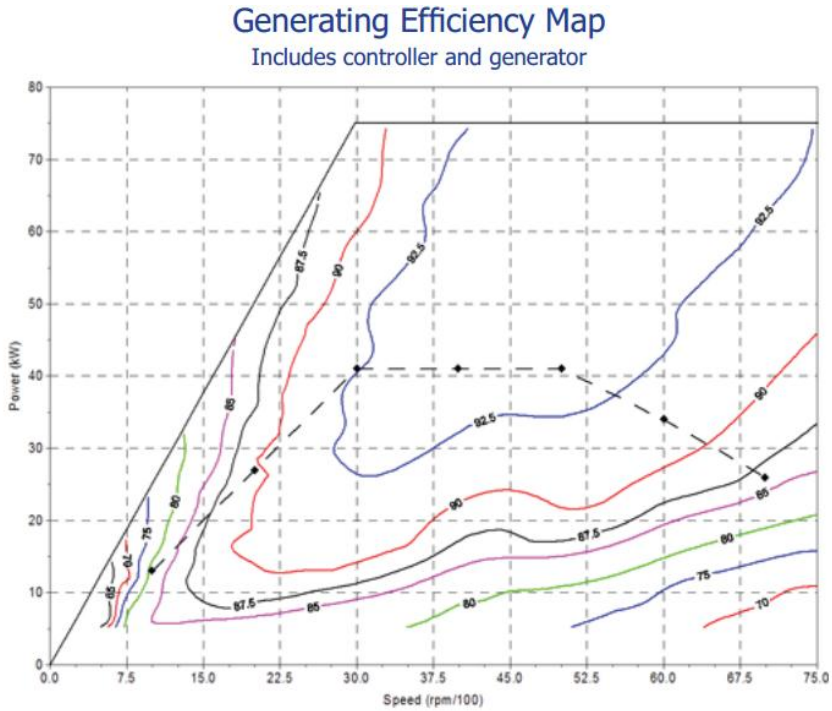

Figure 2-3. Contour plot of generating efficiency map from user manual [11]

2.3 Vehicle Interface

As a part of the PHEV, the APU interacts with other vehicle subsystems and the master vehicle controller. Operation of the APU is tied especially closely to the energy storage system (battery pack).

2.3.1 Energy Storage System

The battery pack is the main energy storage device. The energy storage system (ESS) can be charged by the APU, and the ESS will provide power for Electric Traction System (ETS). Figure 2-4 shows the relationship between the APU, the electric traction system and the energy storage system.

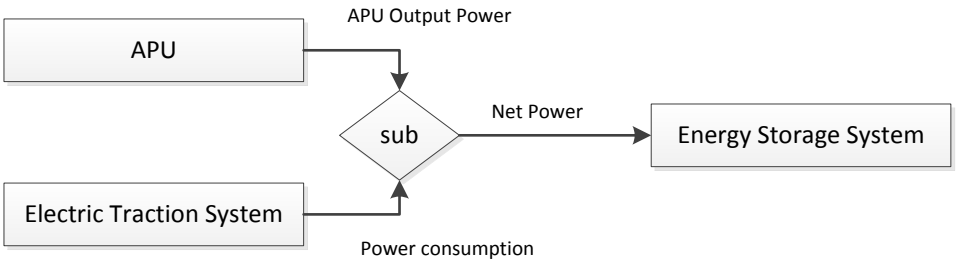

Figure 2-4. The relationship between the APU, the ETS and the ESS

The APU has three operation set points, which will set the engine run at different throttle and speed. The battery SOC will determine which set point will be activated. The low set point is activated below 35% SOC and continues to run until the SOC exceeds 45%. When the SOC is below 25%, the high set point is activated. The SOC range of the high set point is from 7% to 25%. The critical set points will be active when the SOC is less than 7%. This set point runs the APU at nearly the maximum power available to sustain operation of the vehicle at a critically low SOC.

This control strategy is easy to implement and can help us estimate output power of the APU accurately. However, this strategy may not allow the engine to run in its high efficiency speed and torque region. Therefore, the fuel consumption and emission of the engine may not be optimal.

2.3.2 Master Vehicle Controller

The APU collects/sends data and commands via CAN bus from/to the master vehicle controller.

The CAN bus was developed by BOSCH as a multi-master, message broadcast system that specifies a maximum signaling rate of 1 megabit per second (bps). Unlike a traditional network such as USB or Ethernet, CAN does not send large blocks of data

point-to-point from node A to node B under the supervision of a central bus master. In a CAN network, many short messages like temperature or RPM values are broadcast to the entire network, which provides for data consistency in every node of the system. [12] The AVT's controller network is based upon the CAN 2.0b standard. The transmission speed of the network is 500 kbps.

The vehicle controller collects information on battery SOC, current generator/engine speed, engine switch status, engine temperature and etc. via CAN bus. The APU control algorithm within the vehicle controller uses this information to calculate generator/engine speed request, throttle request, generator torque limit and etc., and send the results back to the CAN bus. The vehicle controller can use the results to control the engine and the generator.

Chapter 3

Auxiliary Power Unit Model

The purpose of modeling the Auxiliary Power Unit (APU) is twofold. First, for the purpose of vehicle-level simulation and control, it is necessary to model power output and fuel consumption. Second, for the purpose of APU control, it is necessary to model APU operation mode, startup and shut off condition.

The APU model has three subsystem blocks: IC Engine block, APU generator block, and the APU generator speed control block. These three blocks are shown in the Simulink block diagram of Figure 3-1. In this particular block diagram, Simulink Go To and From blocks are used to avoid busy signal routing. The IC engine block will output the engine torque and calculate the actual engine speed and fuel consumption. The APU generator block will calculate the generator torque and APU output power. The APU generator speed control block is a PI control loop, which will output torque control message according to the error between the speed command and actual speed. Each of these blocks is described in a subsequent section.

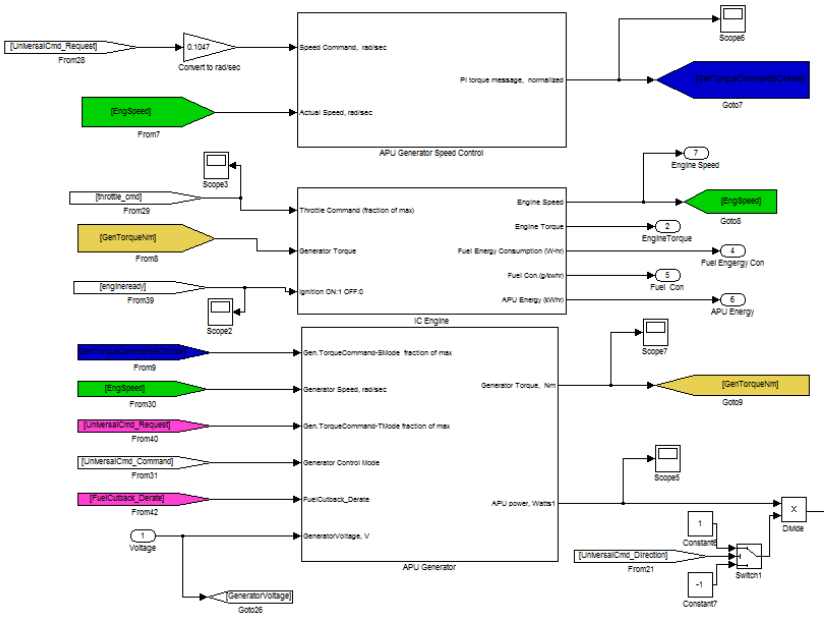

Figure 3-1. APU model

Figure 3-2 shows the flow chart of the APU model.

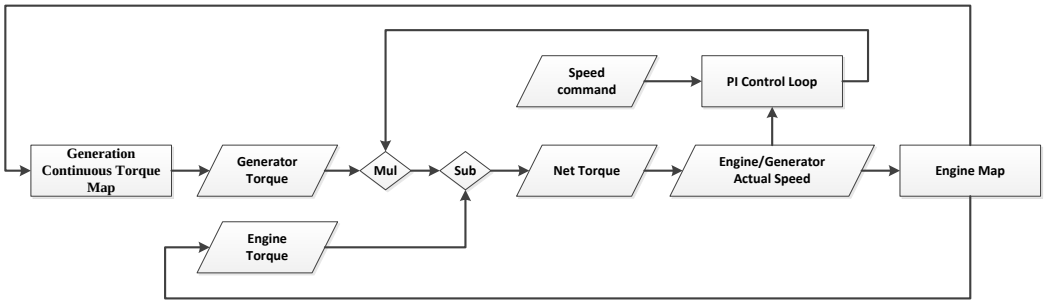

Figure 3-2. The flow chart of APU model

The PI control loop in the model is used to minimize the error between the actual and commanded generator speed. The output control variable of the PI controller will continue to adjust the output generator torque until the actual speed of the generator stabilizes as desired. As long as the actual speed of the generator stabilized, the generator torque and engine torque can be obtained, as well as the output power of the generator and fuel consumption. Therefore, this PI control loop is the key to calculate the output power and fuel consumption.

3.1 Engine Model

Figure 3-3 shows the engine model in Simulink. The primary inputs are the Generator Torque and the Throttle Command; the Ignition input indicates if the engine is running and thus enables/disables the throttle input. The primary outputs are Engine Speed and Fuel Consumption. The Generator Torque is needed to calculate the net torque and the engine speed. The Engine Speed can be calculated by this formula: $\text{engine speed} = \int \frac{\text{Net Torque}}{\text{flywheel inertia}}$. The Throttle Command shows the percentage of the throttle open. The Engine Speed and Throttle Command are used to calculate the Fuel Consumption. Two saturation blocks are used in the model to ensure that the inputs to the engine map are within valid ranges. The engine speed saturation limits are 650 rpm and 7000 rpm. The throttle saturation limits are 0 and 100.

There are three main parts of the engine model – engine speed calculation, engine torque calculation, and fuel consumption calculation.

A significant advantage of the series HEV is the ability to operate the engine independently of vehicle speed/load. The engine can be operated in a region of high efficiency and low emissions. The IC engine model for the series HEV is simpler than that required for an ICE vehicle as it does not need to model idle conditions [13].

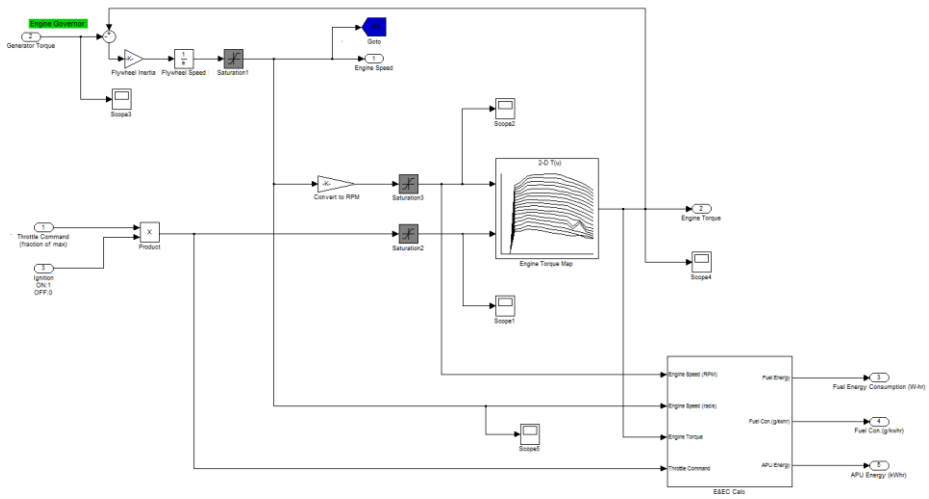

Figure 3-3. Engine model

3.1.1 Torque Map

The engine map is a simple, static model of the engine. It provides the power or torque delivered by the engine as a function of engine speed and engine throttle position. The relationship between engine torque and engine power is: $Torque = \frac{\text{Power(W)}\times 60}{2\pi \times RPM}$. In this study, the map describes the engine output power or torque relative to the engine speed and engine throttle. This is a 2-dimensional table with engine speed and throttle as inputs and power/torque as output. This map was defined by point-by-point test and interpolation method.

3.1.1.1 Physical Test

An engine dynamometer was used to find some points of the map. Figure 3-4 shows the engine dynamometer platform.

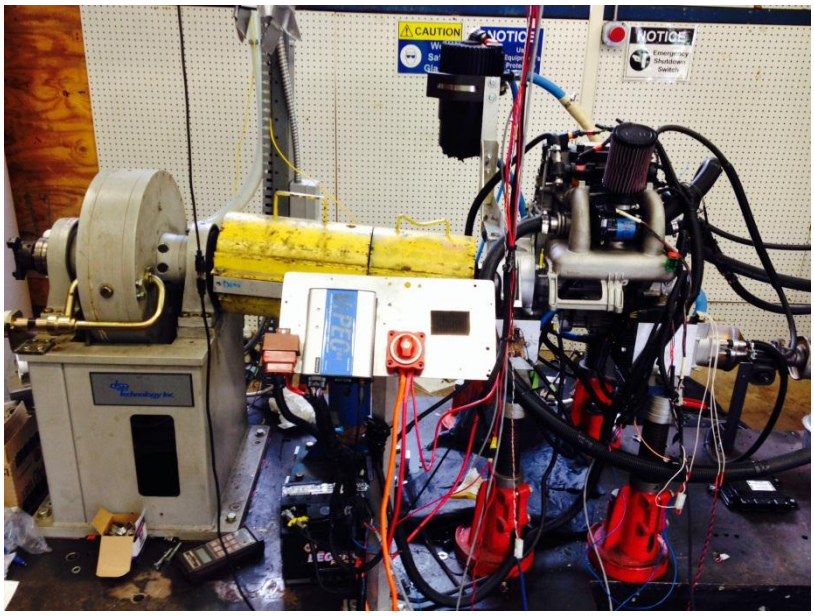

Figure 3-4. Dynamometer platform

Table 3-1 shows the data obtained from the dynamometer test.

	2000 rpm	2500 rpm	3000 rpm	3500 rpm
1% Throttle	3 kW	1.8 kW	0 kW	0 kW
3% Throttle	4.5 kW	3.6 kW	1 kW	0 kW
5% Throttle	5.8 kW	4.7 kW	3 kW	1 kW
10% Throttle	7.2 kW	7 kW	7 kW	5 kW
20% Throttle	9 kW	10 kW	12 kW	11.2 kW
30% Throttle	9.8 kW	12 kW	13.5 kW	14 kW
40% Throttle	10.7 kW	12.5 kW	15 kW	16.8 kW
50% Throttle	10 kW	13.5 kW	16 kW	18 kW
70% Throttle	10.8 kW	14.5 kW	18.5 kW	21 kW
80% Throttle	11 kW	14.4 kW	19 kW	23 kW
90% Throttle	10.8 kW	14.3 kW	19 kW	23 kW
100% Throttle	10.8 kW	14.1 kW	20 kW	24 kW

Table 3-1. Engine map from dynamometer

The Penn State vehicle was also sent to have an emissions and fuel economy test in a controlled laboratory environment in Ohio. Subsystem testing was performed and the engine has been tuned. Because the testing speed range of engine was from 3000 rpm

to 4500 rpm and the throttle range was between 20% and 40%, 12 points were tested and available in the map. The following table is the tuned engine table.

	3000rpm	3500rpm	4000rpm	4500rpm
20% Throttle	14 kW	17.5 kW	19 kW	21 kW
30% Throttle	14.5 kW	18 kW	19.8 kW	23 kW
40% Throttle	15 kW	19 kW	21 kW	24 kW

Table 3-2. The tuned engine map

3.1.1.2 Interpolation

Measurement of the engine map is excessively time consuming if the engine must be operated at a large number of points. If we set the interval of RPM to 50 and the interval of throttle to 1%, there are 12928 points that must be measured. However, if the range of RPM data is from 3000 to 4500 and the interval is 500, and the range of throttle data is from 20% to 40% and the interval is 10%, only 12 points are needed. Interpolation can be used to get the rest of the points. Interpolation is a method of constructing new data points within the range of a discrete set of known data points [1].

Three interpolation methods are commonly used.

1. Linear interpolation

It is one of the simplest interpolation methods. It is a method of curve fitting using linear polynomials. The interpolant at point (x,y) is:

$$y = y_a + (y_b - y_a)\frac{x - x_a}{x_b - x_a}$$

Because the engine map is a 2-demension map, bilinear interpolation method, which is an extension of linear interpolation for interpolating functions of two variables on a regular 2D grid [1], is used. Bilinear interpolation method utilizes linear interpolation in both the x-direction and y-direction.

2. Nearest interpolation

Nearest interpolation method selects the value of the nearest point and does not consider the values of neighboring points at all.

3. Cubic spline interpolation

Spline interpolation is a method form of interpolation where the interpolation is a special type of piecewise polynomial called a spline [1]. The separate polynomials pass through each interval of each of the given values, each polynomial has its own coefficients. Each polynomial can be represented like this:

$$S_i(x) = a_i(x - x_i)^3 + b_i(x - x_i)^2 + c_i(x - x_i) + d_i$$

Because each polynomial has four coefficients, each segment requires four points to define the coefficients. Two endpoints of the segment and the two points on either side of them are used to fix the polynomial.

These three methods fill out the torque map, make the output curve become smooth and reduce the error.

3.1.1.3 Comparison

Figure 3-5 shows the comparison of original engine map and other three expended engine map of the engine.

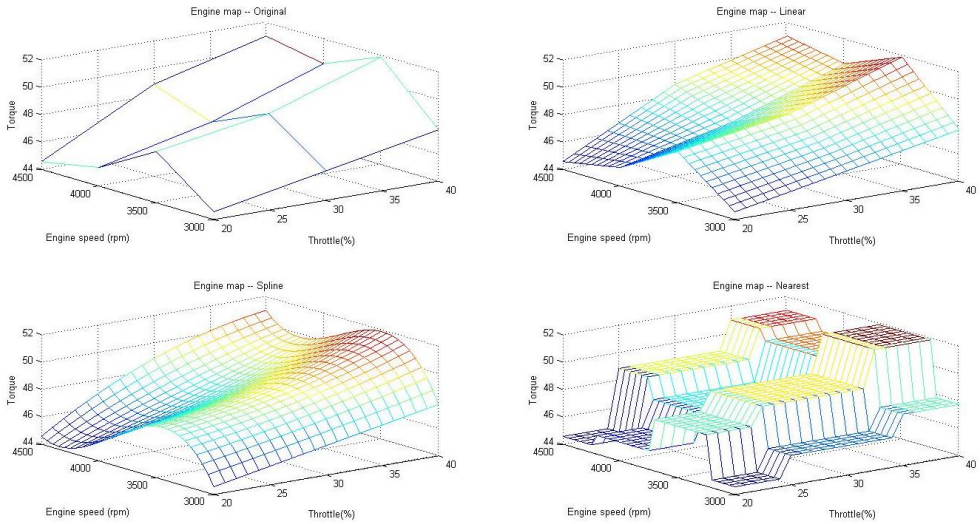

Figure 3-5. Comparison of original engine map and three expended engine maps

The Figure 3-5 shows that all three expended efficiency map can help us find more reasonable data and can make the mesh smooth. However, the plots of linear interpolation method and spline interpolation method are closer to the original efficiency map.

3.1.2 Brake Specific Fuel Consumption Map

The energy and energy consumption calculation block (Figure 3-6) is used to calculate the APU energy, fuel energy, and fuel consumption. The Brake specific fuel consumption (BSFC) map is used to find the fuel energy and fuel consumption. With the engine speed, engine torque, and the BSFC map, the fuel consumption can be found.

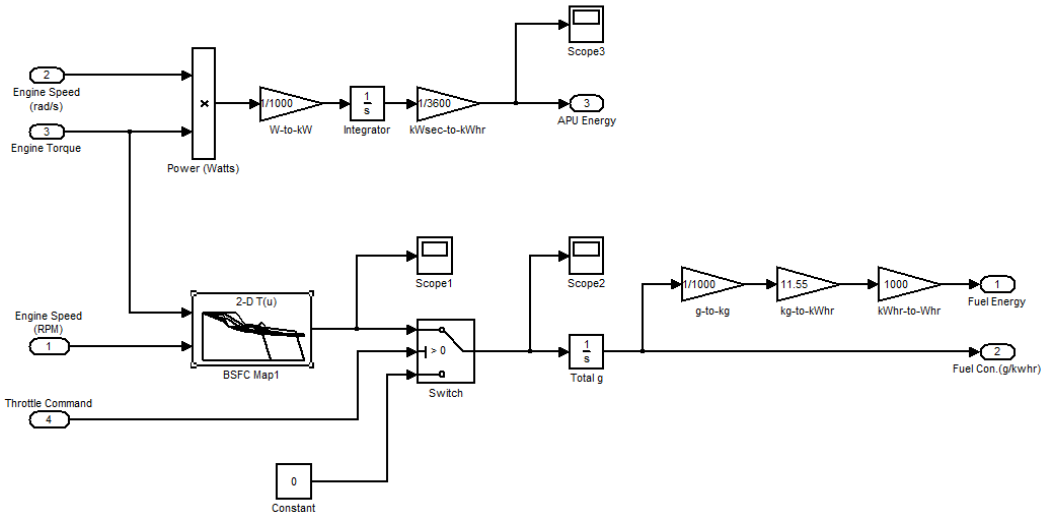

Figure 3-6. Energy and energy consumption calculation block

Engine power can be calculated by multiplying Engine Speed and Engine Torque because $P(kw) = \frac{Torque(Nm) \times Speed(rad/s)}{1000}$. Figure 3-7 is the BSFC map plot. This BSFC shows the relationship among the throttle, speed and the fuel consumption and can help us to find some points which have less consumption.

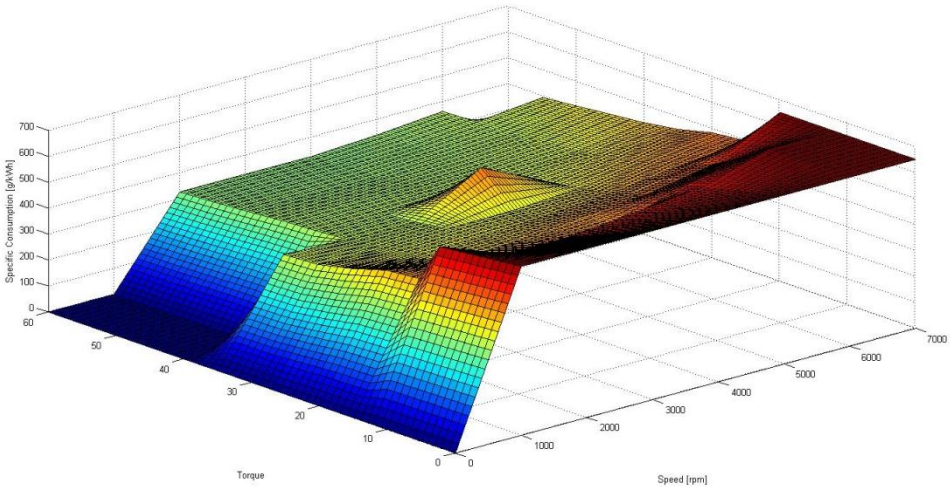

Figure 3-7. Plot of Weber MPE 750 BSFC map.

3.2 Generator Model

The engine of the vehicle often varies its speed to match the command from the vehicle controller. The generator will use the engine as the prime mover in this project, so the output current from the generator's alternator will have fluctuations. To eliminate fluctuations, the ac power produced by the generator's alternator will be converted to dc power. Then the inverter will cover the dc power back to ac power. Therefore, the smooth and clean 3-phase current can be obtained after the conversion.

The UQM controller will control the conversion process, as well as the generator speed.

Figure 3-8 shows the generator model in Simulink. The primary inputs are the Torque Command and Generator Speed. The primary outputs are Generator Torque and APU Power. The Torque Command is the control variable of the PI control loop. It is needed to calculate the Generator Torque output. The Generator speed is used to find the generator power losses, APU power, and continues generator torque.

There are two main parts of the generator model – APU power calculation and generator torque calculation.

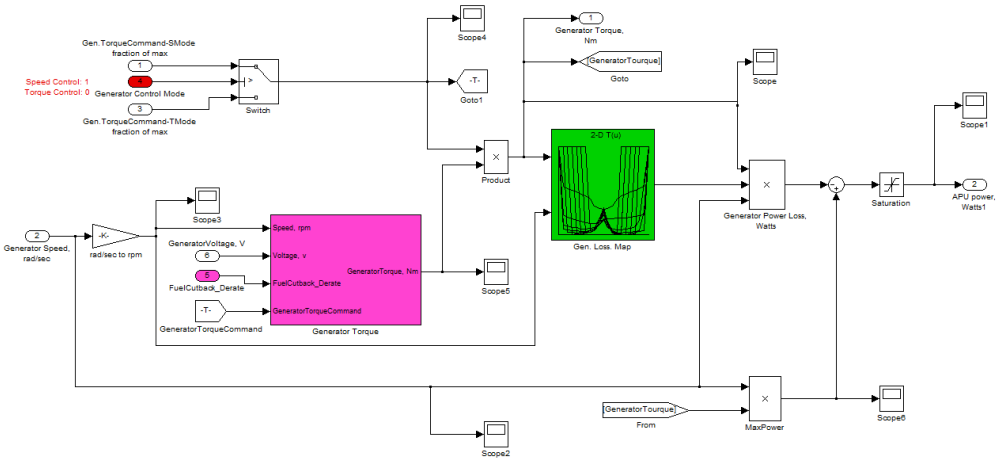

Figure 3-8. Generator model

3.2.1 Torque Block

The generator torque calculation block (Figure 3-9) is in the generator model. This block is used to find the generator torque.

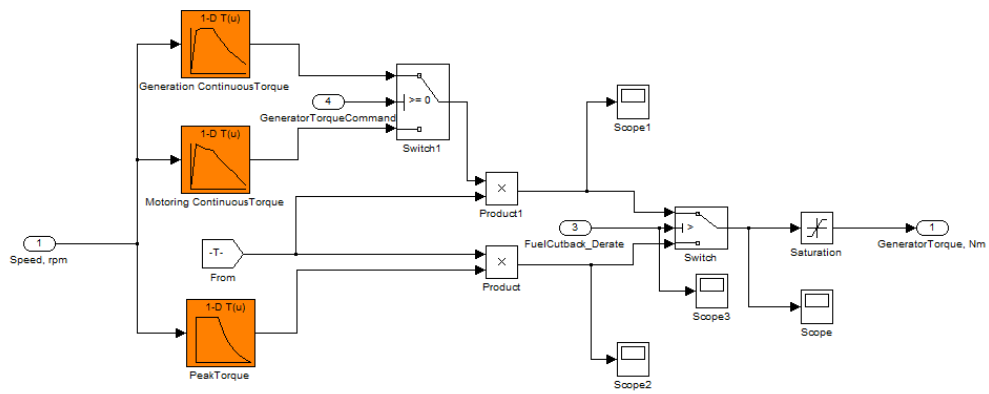

Figure 3-9. Generator torque calculation block

Three maps are used in this block. They are generation continuous torque map, motoring continuous torque map and peak torque map. Because of $P(kw) = \frac{Torque(Nm) \times Speed(rad/s)}{1000}$ and $1\,rad/s = \frac{60}{2\pi}\,RPM$, the relationship of speed and torque shown in Table 3-3. UQM Technologies provides these three maps [10].

Speed (RPM)	Generating Continuous Torque	Motoring Continuous Torque	Peak Torque
1000	120.37	160	238.73
2000	125.00	150	238.73
3000	126.54	140	238.73
4000	94.91	110	173.61
5000	75.93	84	138.89
6000	53.47	60	115.74
7000	34.39	28	99.2

Table 3-3. Continuous torque map and peak torque map

3.2.2 Generator Power Losses Map

The generator power losses map models the power losses when the generator converts the power from mechanical to electrical. It represents the efficiency of power transformation in different generator speed and generator torque. This is a 2-dimension table with generator speed and generator torque as inputs and power losses as output. The data of this map was provided by manufacturer.

3.2.2.1 Original Data

The efficiency data table of UQM generator provided by UQM Technologies shows that the values of independent variables form an unstructured mesh rather than a regular mesh. To get the contour plot of the efficiency map like the Figure 2-3, Delaunay triangulation was created (Figure 3-10).

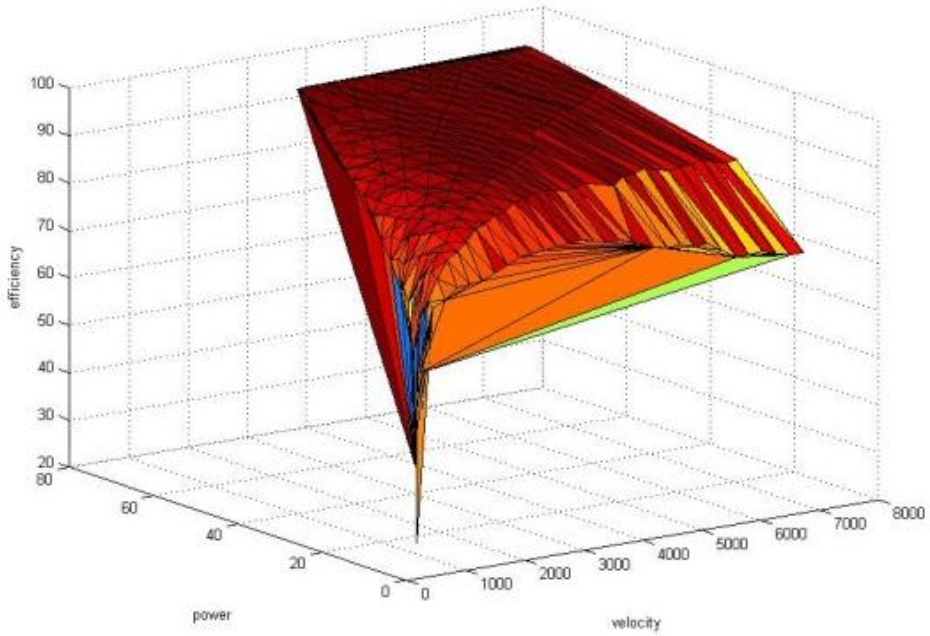

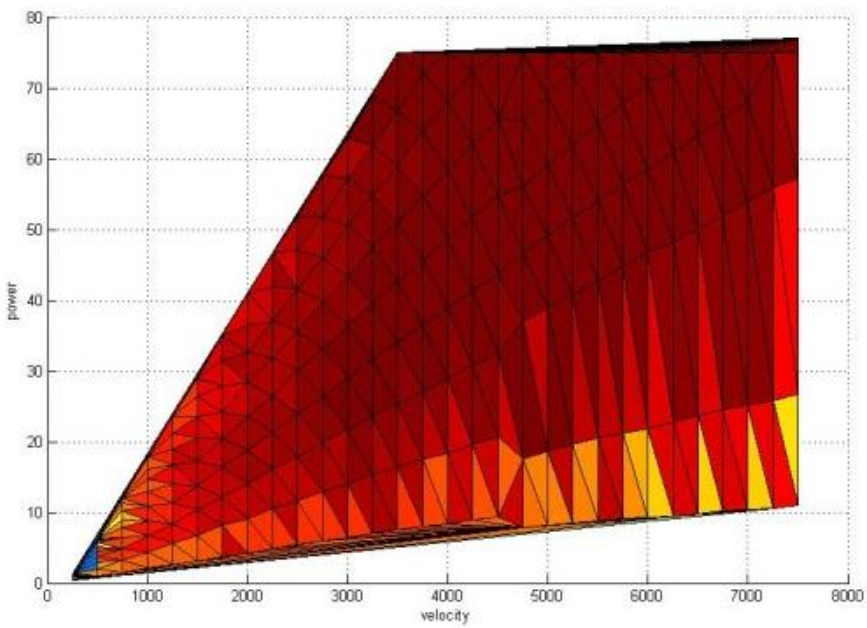

Figure 3-10. Delaunay triangulation plot of efficiency Map

The uniform mesh can be generated by going through triangles and interpolate points. Then the efficiency map can be plotted. Figure 3-11 illustrates the efficiency map of the generator

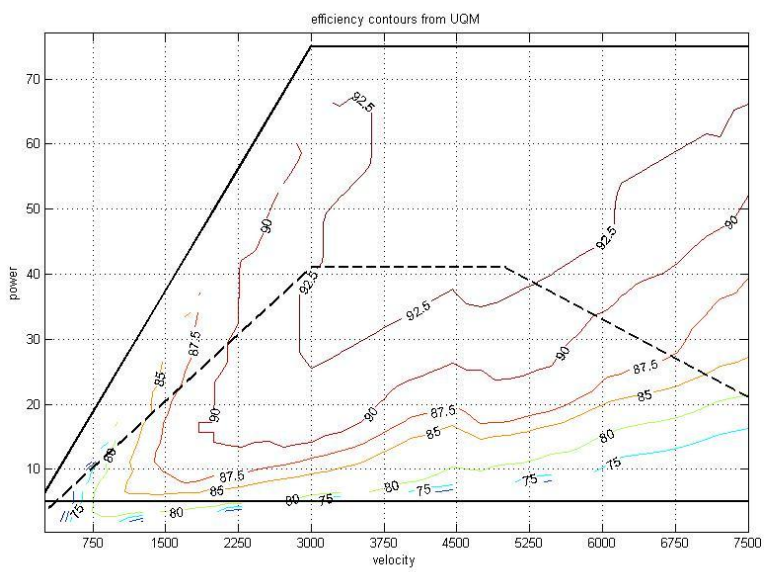

Figure 3-11. Contour plot of generating efficiency map from data table

Comparing Figure 3-11 to Figure 2-3, the plot in the Figure 3-11 does not match the Figure 2-3 well. So the method of collecting data from Figure 2-3 is used. Table 3-4 shows the efficiency table.

RPM / Power	0	750	1500	2250	3000	3750	4500	5250	6000	6750	7500
0	66	76	77	78	78	76	72	69	68	66	64
10	40	75	88	88	86	83	80	78	75	72	70
20	50	70	87	90.5	90.5	90	88.5	89	85.5	82	79
30	0	70	83	90.5	92.5	92.5	92.5	91.5	90.5	89	86.5
40	0	70	82	89.5	92.5	92.5	92.5	92.5	92	91	89
50	0	0	80	87.5	91.5	92.5	92.5	92.5	92.5	91.5	90.5
60	0	0	78	86	90	92.5	92.5	92.5	92.5	92.5	91.5
70	0	0	0	84	89	92	92.5	92.5	92.5	92.5	92
80	0	0	0	77	88	91	92.5	92.5	92.5	92.5	92.5

Table 3-4. Efficiency data table

Then contour plot of efficiency map is plotted and shown in the Figure 3-12.

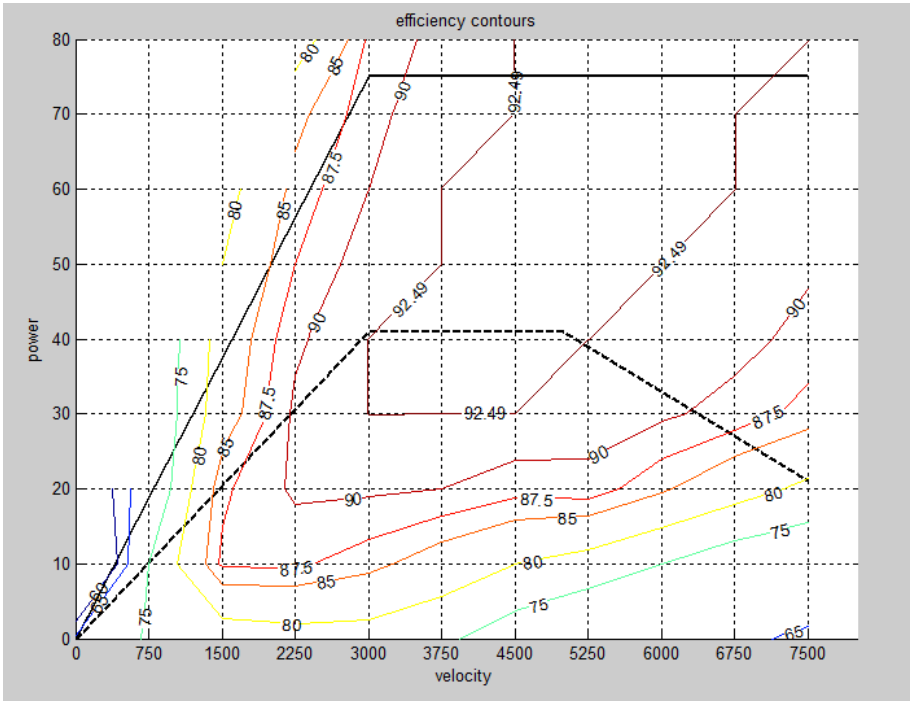

Figure 3-12. Contour plot of generating Efficiency Map

Compare the Figure 3-12 to the Figure 3-11, the Figure 3-12 is more accurate. However, a great error will still occur if this efficiency map is used because the data in the lookup table is not enough. The gap between each point causes the inaccurate output. Therefore, interpolation methods to optimize the efficiency map are used.

3.2.2.2 Interpolation

Three interpolation methods, linear interpolation, nearest interpolation and spline interpolation, are used.

With these three expended efficiency data table, the contour plot of efficiency map of generating can be plotted (Figure 3-13).

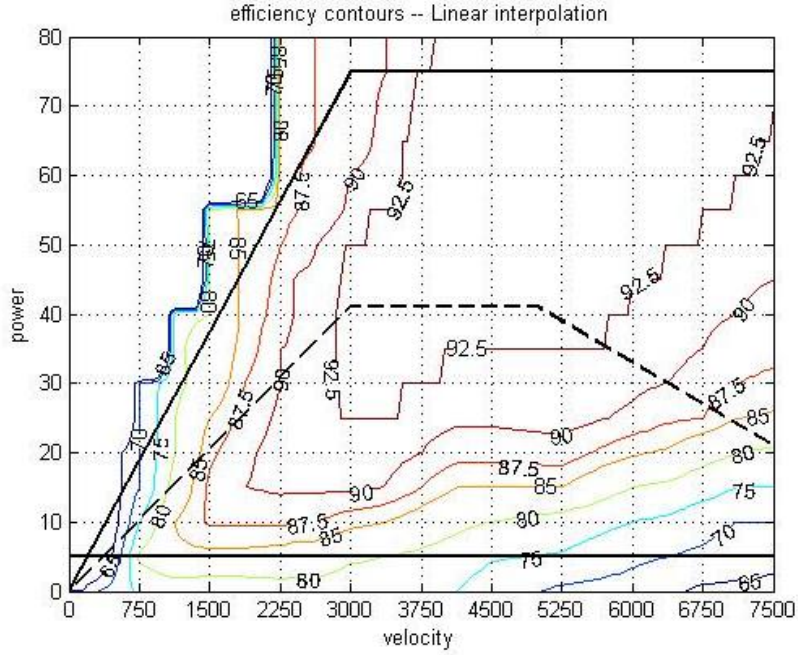
efficiency contours -- Linear interpolation
power
velocity
0
10
20
30
40
50
60
70
80
0
750
1500
2250
3000
3750
4500
5250
6000
6750
7500

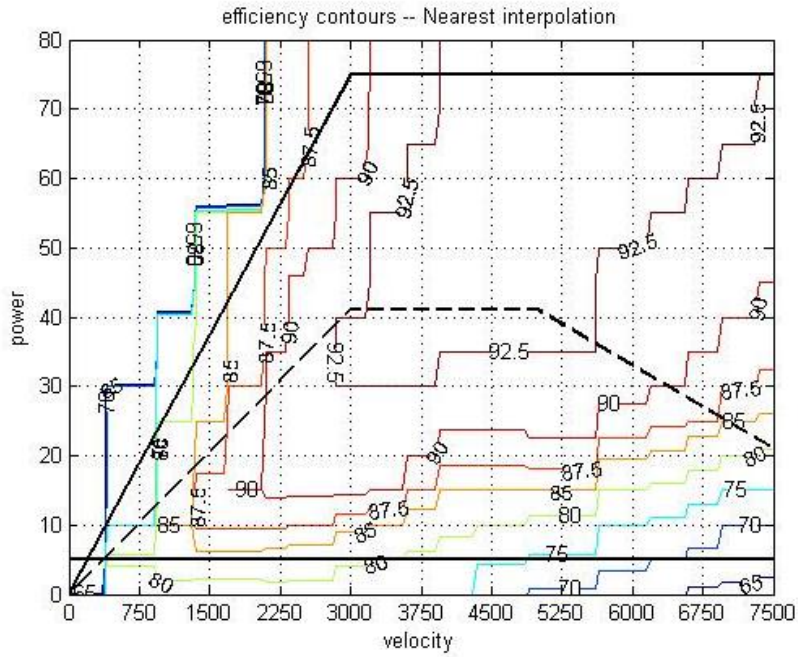
efficiency contours -- Nearest interpolation
power
velocity
0
10
20
30
40
50
60
70
80
0
750
1500
2250
3000
3750
4500
5250
6000
6750
7500

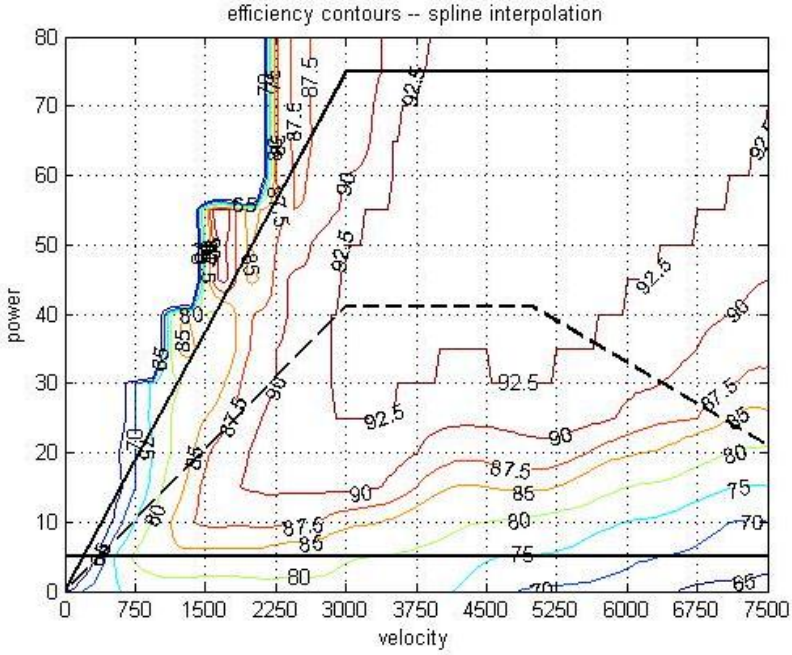

Figure 3-13. Contour plot of three expended efficiency data map

3.2.2.3 Comparison

Figure 3-14 shows the comparison of original efficiency map and other three expended efficiency map of the generator.

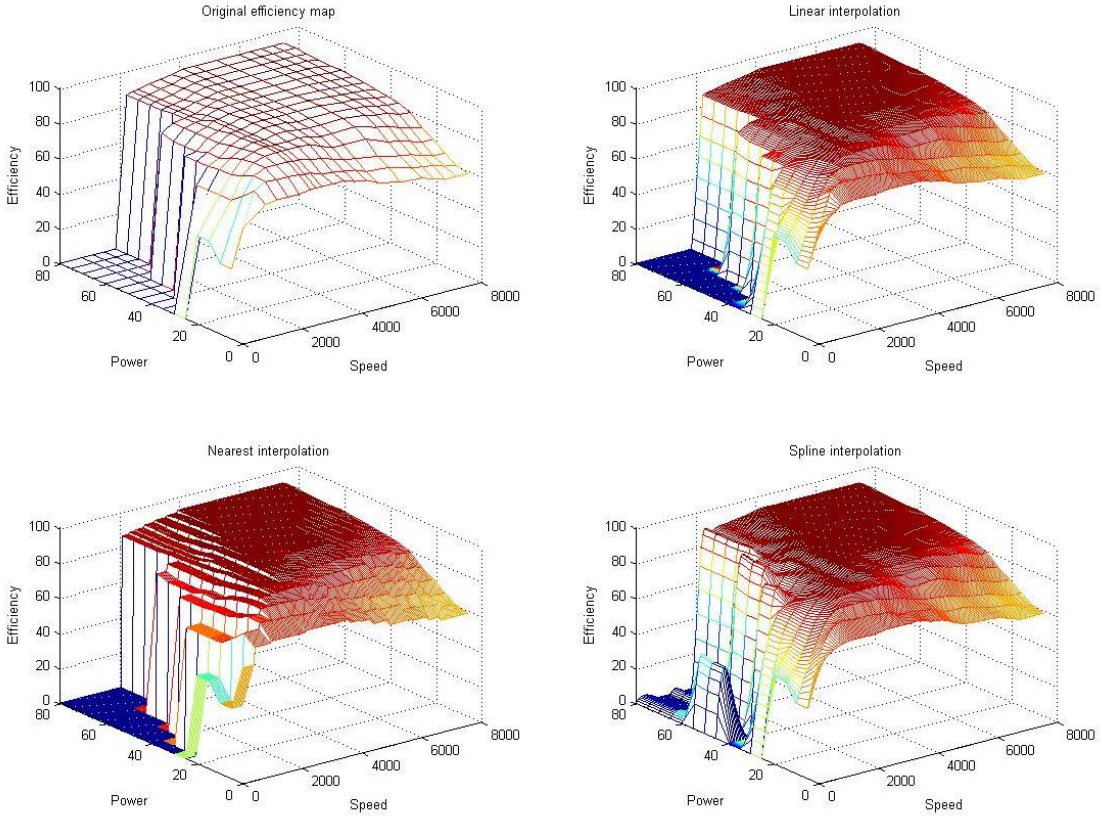

Figure 3-14. Comparison of the original and the expended efficiency data maps

Both the Figure 3-13 and the Figure 3-14 show that all three expended efficiency map can help us find more reasonable data and can make the mesh smooth.

3.3 Generator Speed Control Block

The output of the generator speed control function block (Figure 3-15) is used as the “generator torque command speed control mode” input of the generator model.

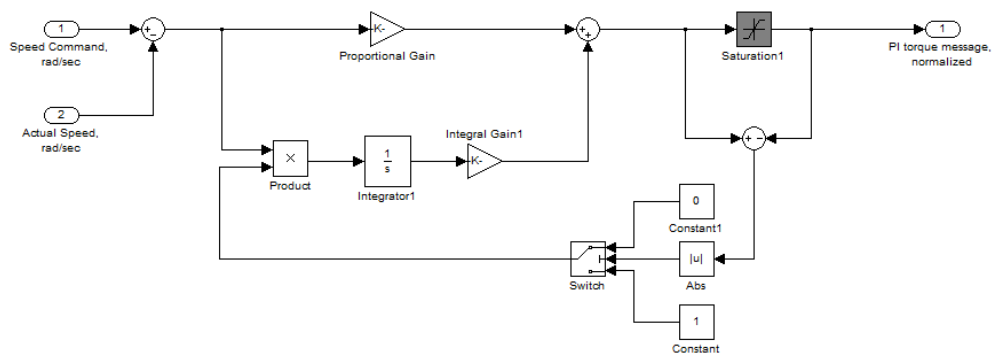

Figure 3-15. Generator speed control function block

The block uses PI close control loop to calculate the normalized torque message. The PI loop has an anti-windup mechanism. The windup will occurs when the output of the PI loop exceeds the limitation of the actuator and comes into the saturation region. The PI controller is unable to immediately leave the saturation and respond to changes in the error because of the integral part of the PI loop. The anti-windup mechanism will prevent windup. The PI loop will forbid the integral part when the output of the PI loop in the saturation region, so that the PI controller can recover faster when the error changes sign.

The Ziegler–Nichols method is used to calculate the gain of the PI loop. Firstly, the proportional band is narrowed down in the proportional control mode to determine the proportional band (K_u) and period of oscillation (P_u). Since $\mathrm{K}_P = 0.45K_u$ and $\mathrm{K}_I = 1.2K_P/P_u$, the K_P and K_I can be calculated.

Figure 3-16 shows the output when $\mathrm{K}_u = 0.13$ and $\mathrm{P}_u = 100ms$. Therefore, the calculated $\mathrm{K}_P = 0.059$ and $\mathrm{K}_I = 0.0007$

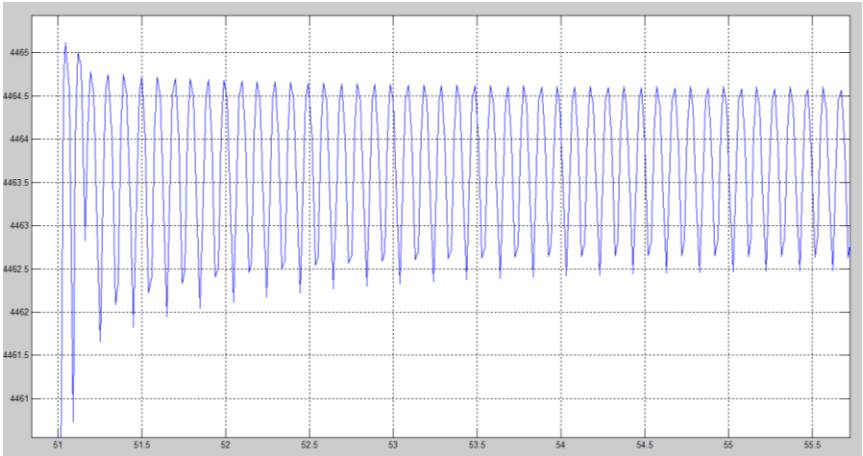

Figure 3-16. Output of PI loop

In this project, the gain of P is 0.05 and the gain of I is 0.0015. In the original model, because the lack of trace data, the model was using the approximated gain of P, which is 0.1, and the approximated gain of I, which is 0.00089.

Chapter 4

Auxiliary Power Unit Control

The APU plays a significant role in energy saving and emission reduction for a series PHEV. An effective control strategy can make the APU run steadily in a region of high efficiency and low emission. Therefore, once a model of the APU has been established, the control scheme is of utmost priority. In the following, the control scheme is explained.

4.1 Introduction

The series PHEV architecture permits electric-only operation of the vehicle for the majority of the ESS's capacity. The auxiliary power unit sustains the ESS state of charge for continued operation. Therefore the control strategy and algorithm of APU will have great effect on the power output, fuel consumption and emission of the vehicle.

The APU runs intermittently. More specifically, it will be turned on & off depending on the battery state of charge (SOC).

$$\mathrm{SOC} = \frac{C_{max} - C_{used}}{C_{max}}$$

Figure 4-1 shows the block diagram of the APU controller.

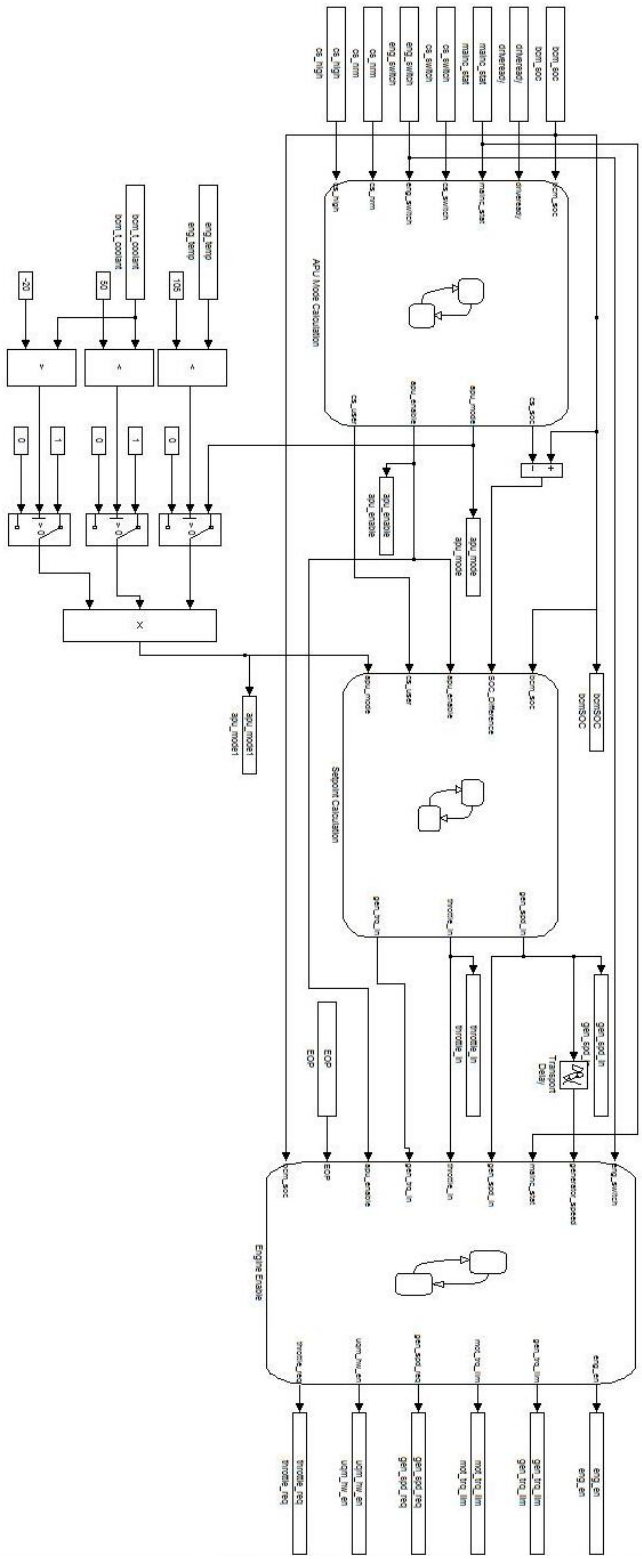

Figure 4-1. APU controller block diagram

The APU controller block diagram consists of three subblocks.

- APU mode calculation
  Determine APU mode and enable & disable APU.
- Set points calculation
  Determine generator/engine speed and throttle values based on the APU mode and battery pack SOC.
- Engine control
  Enable & disable and control the engine, and set engine speed and throttle.

The engine status depends on the battery SOC and three set points. Therefore, APU mode and set points need to be calculated and they will determine if the engine needs to be switched on or off and what the engine speed and throttle should be.

4.2 APU Mode and Operation Determination

The Weber MPE 750 engine will be turned on when the battery SOC lies less than the setting SOC, or when the charge sustaining switch is on or the engine switch is on. In addition, the engine speed is determined by set points and battery SOC as well.

4.2.1 APU Mode Calculation

Figure 4-2 shows how the APU modes are determined. The battery SOC, charge sustaining switch and engine switch are the three most important transition conditions. The Engine Charge mode and Engine On mode will only be selected when the engine switch is ON. The Charge Sustaining mode will be selected when the battery SOC is low, or the charge sustaining switch is ON. Otherwise, the APU will run in the Charge Depletion mode (electric traction motor using only the ESS's stored energy from charging).

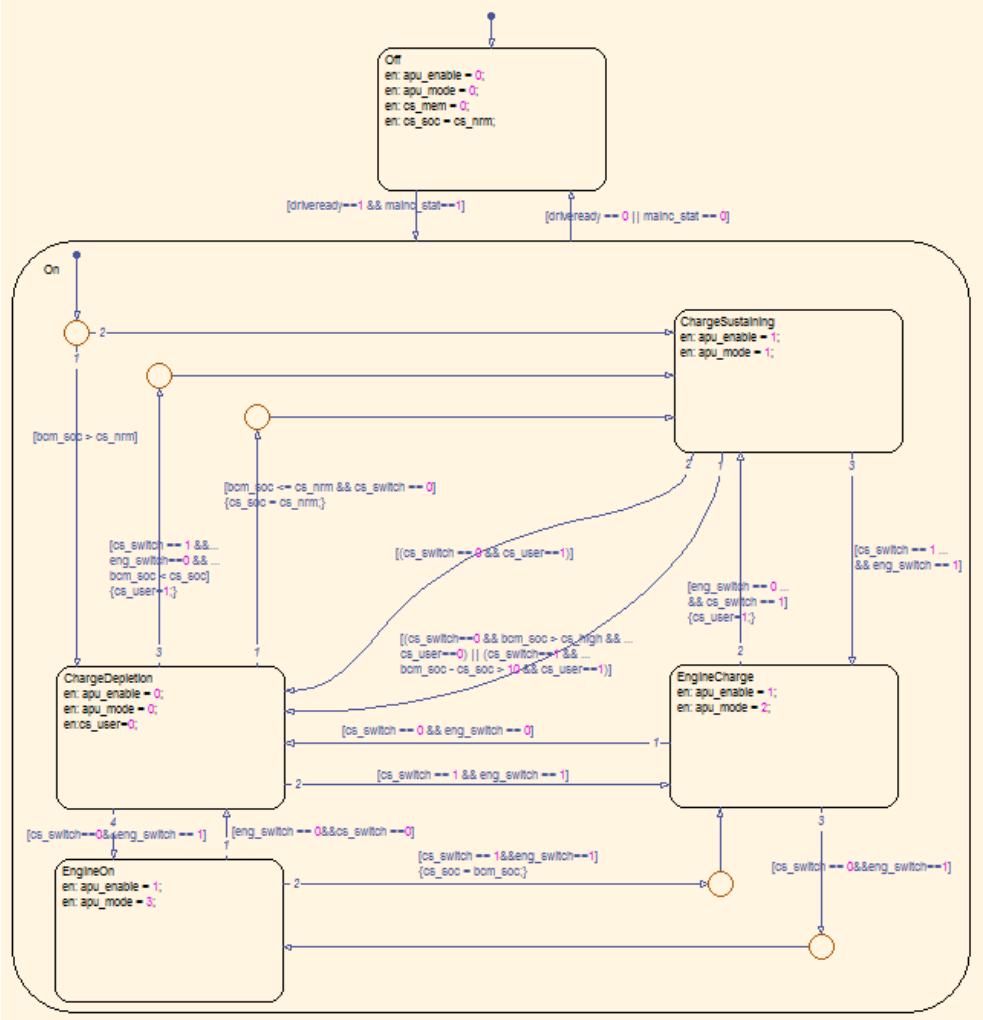

Figure 4-2. State flow of APU mode calculation

The Table 4-1 shows the APU mode in each state.

	APU Enable	APU Mode
Off State	0	0
Charge Depletion State	0	0
Charge Sustaining State	1	1
Engine On State	1	3
Engine Charge State	1	2

Table 4-1. APU mode in each state

4.2.2 Set Point Calculation

The set points calculation block diagram, which is shown in the Figure 4-3, uses the APU enable signal, APU mode and SOC to determine the generator/engine speed request and throttle request.

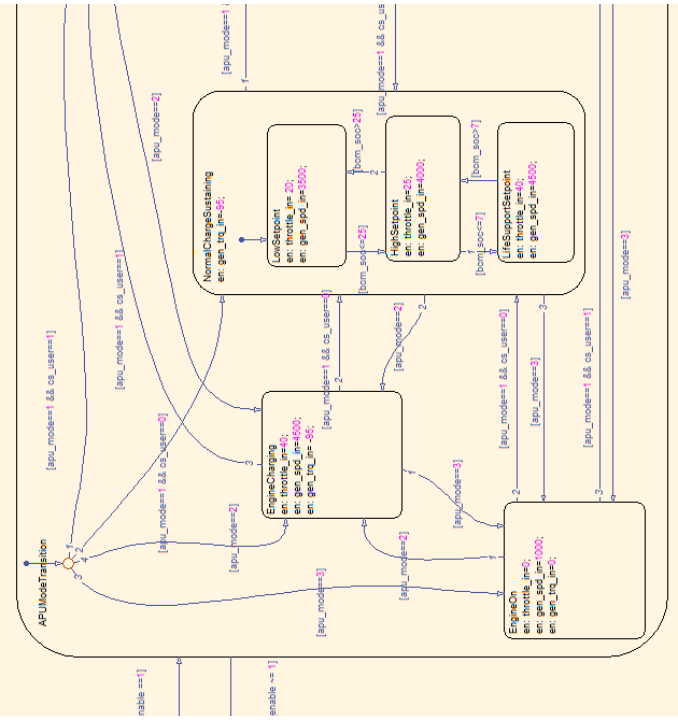

Figure 4-3. APU set points calculation

From the emissions testing event in Ohio, the mean ESS power output of the tested City High Way drive cycle is 15.5 kW. This data can help us to choose set points. In this project, we use this average power as low set point output power, and set the high set point output power 10% higher than the average power. The critical set point runs the APU at nearly the maximum available power to sustain operation of the vehicle at a low SOC.

Three set points are determined. The Table 4-2 shows the speed, throttle and the output power of these three set points.

	Speed	Throttle	Output Power
Low set point	3500 rpm	20%	16 kW
High set point	4000 rpm	25%	17.5 k W
Critical set point	4500 rpm	40%	22 kW

Table 4-2. Set points information

Figure 4-4 shows limits corresponding to engine temperature and battery temperature.

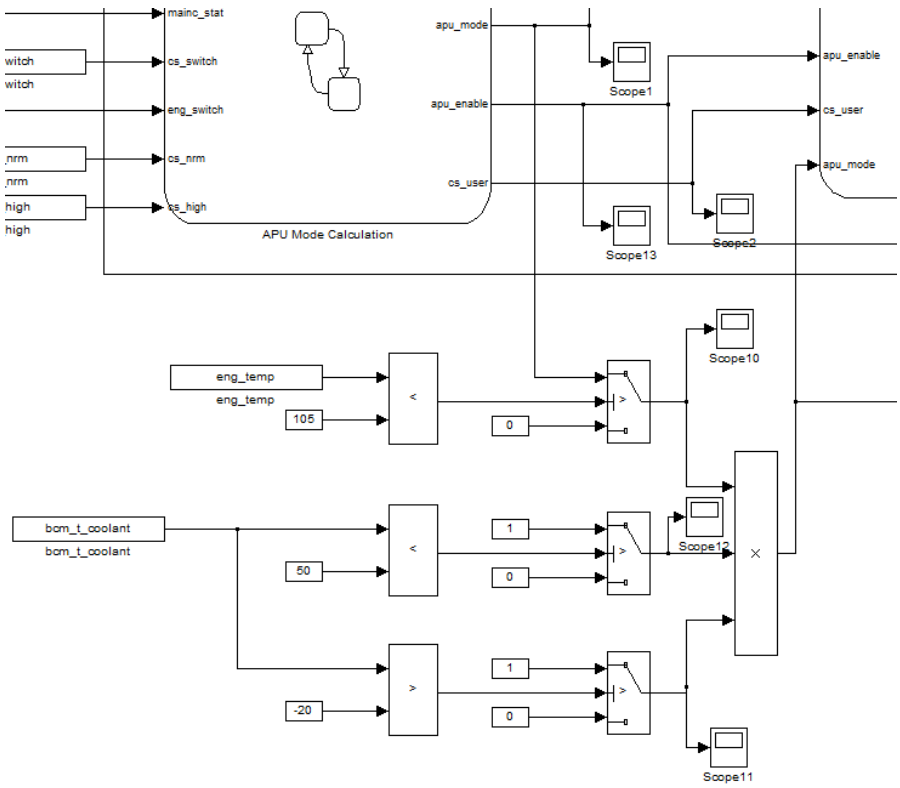

Figure 4-4. The limitation of engine temperature and battery temperature

Before the block diagram output the APU mode, the temperature of engine must be considered because the temperature of the engine is the key constraint on engine power output. Although the engine can limit the power output by itself based on its temperature, the engine temperature limitation is still necessary. Because the engine will be damaged if it limits itself unless we limit it before it does.

The battery pack temperature must also be considered. When the temperature of battery is higher than 50℃ or lower than -20℃, the current drops sharply or even is 0. The best operating temperature of the battery pack is from 10℃ to 50℃ for charging and from 0℃ to 50℃ for discharging.

4.3 Engine Control

Weber MPE 750 engine is operated in intermittently based on the battery SOC and engine switch status.

Figure 4-5 shows the state flow of the engine operation. There are seven state of operation: off state, reset state, startup state, cranking state, transition state, failed crank state and running state.

The block will set the engine speed at 1000 rpm and throttle at 0 and then try to crank the engine. If the generator speed can reach 1200 rpm within 5 seconds, it means the cranking is successful and the engine is running with the speed request value and throttle request value the block got from set points calculation function block. Otherwise, the cranking is failed. The function block will try to startup the engine again.

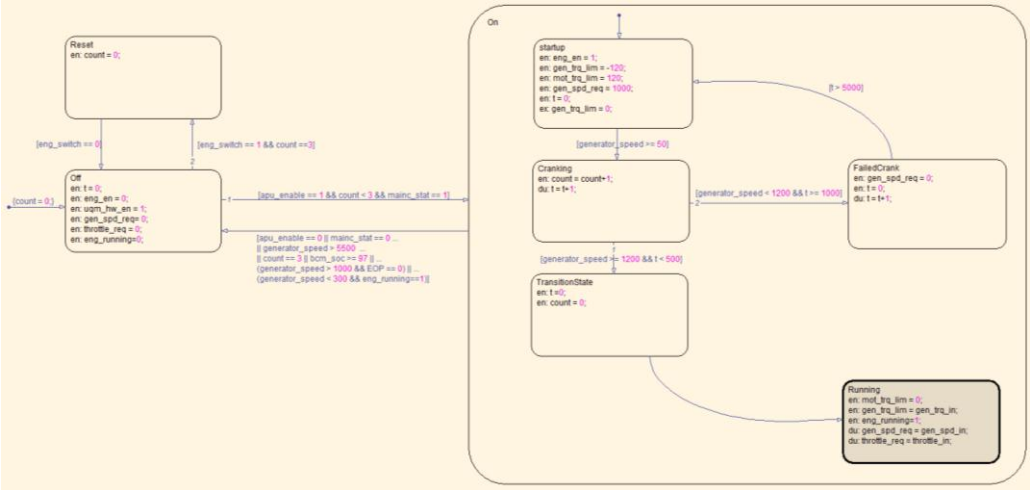

Figure 4-5. State flow of engine operation

The engine control block diagram will start up the engine and issue commanded values for speed and throttle position.

Chapter 5

Auxiliary Power Unit Performance

5.1 Simulation of the Auxiliary Power Unit

The APU was modeled and simulated in Simulink. Simulating the control algorithm facilitates the control scheme implementation and parameters setting because the Master Vehicle Controller can be programmed from a Simulink-based program.

The APU mode calculation block diagram determines APU mode based on the battery SOC, engine switch and charge sustaining switch, and then deliver the APU mode and APU enable signal to the Set Point Calculation block diagram. The Set Point Calculation block diagram determines commanded values for generator/engine speed and throttle position based on the APU mode and battery pack SOC. The commanded values are sent to the APU control block, which will eventually output the command to control the throttle position of the engine, engine/generator speed, engine on & off and etc.

Several simulations of the modeled APU were performed to verify the control strategy. The simulation of submodels is discussed in the following sections of this chapter.

5.1.1 Simulation of APU Model

The vehicle was sent to have an emissions and fuel economy test in a controlled laboratory environment in Ohio. Some data from those tests were used to validate the APU model. Table 5-1 shows the speed and throttle values that were used for the

validation; these correspond to the resulting test data includes generator/engine speed, voltage and current. The generator speed in these datasets is used as a reference speed. A PID control loop is used to make the simulated speed match the reference speed.

	RPM	Throttle
Run 4	3500	20%
		40%
Run 9	3000	20%
		40%
	4500	20%
		40%

Table 5-1. Speed and throttle information of simulation datasets

The Figure 5-1 shows the comparison of reference generator speed and output speed of the APU model when dataset Run 4 is used.

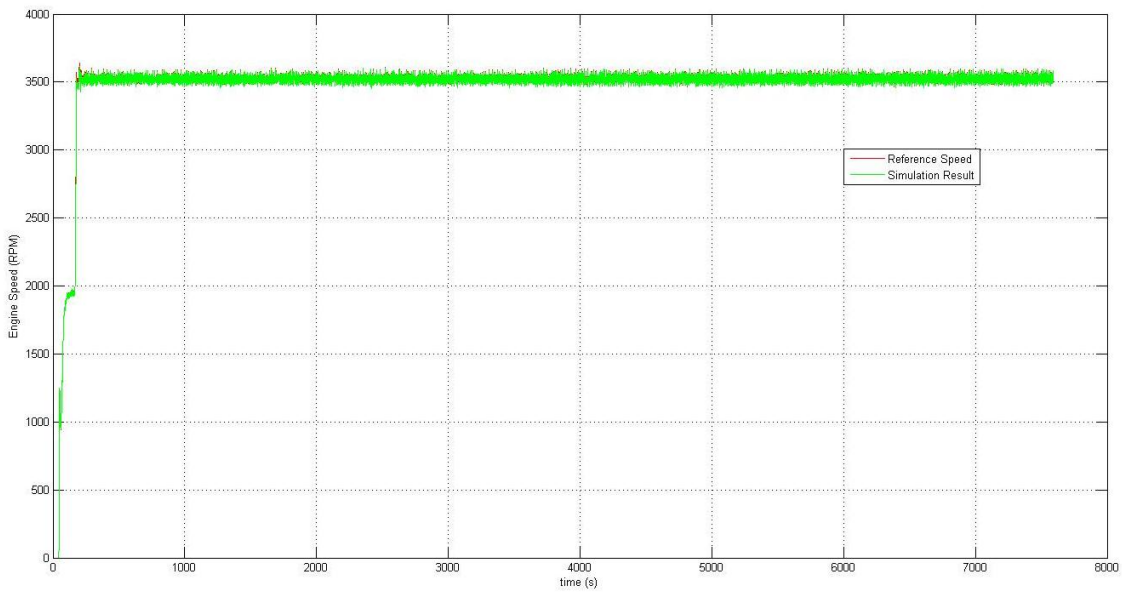

Figure 5-1. Comparison of reference generator speed and simulated generator speed when the Run 4 used

Figure 5-2 shows the comparison of reference output power of generator and output power of the APU model when dataset Run 4 is used.

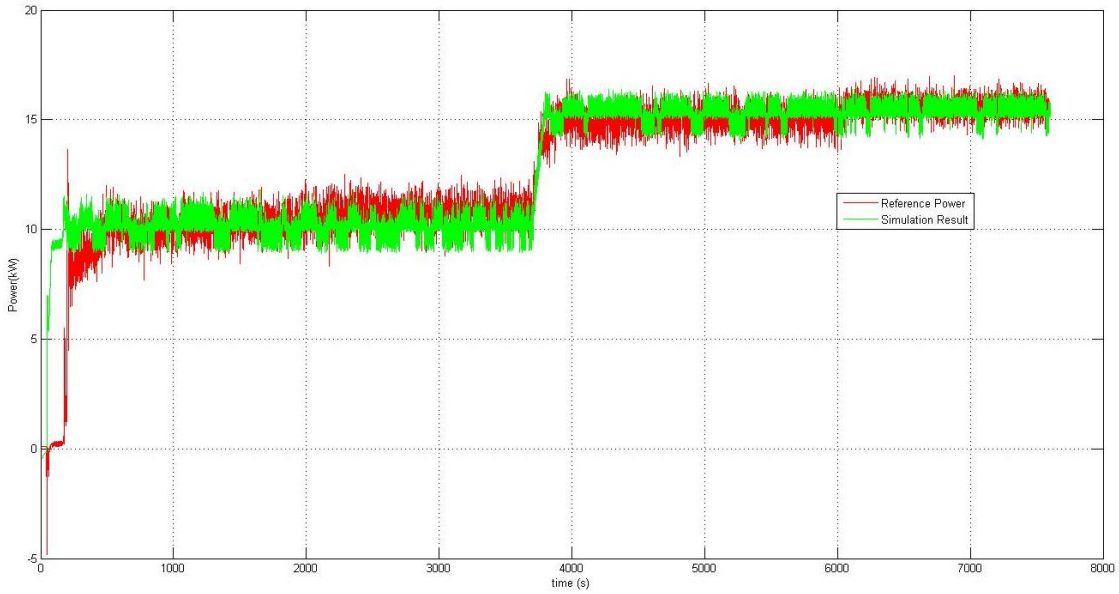

Figure 5-2. Comparison of reference output power of generator and simulated output power of generator when the Run 4 used

The Figure 5-3 shows the comparison of reference generator speed and output speed of the APU model when dataset Run 9 is used.

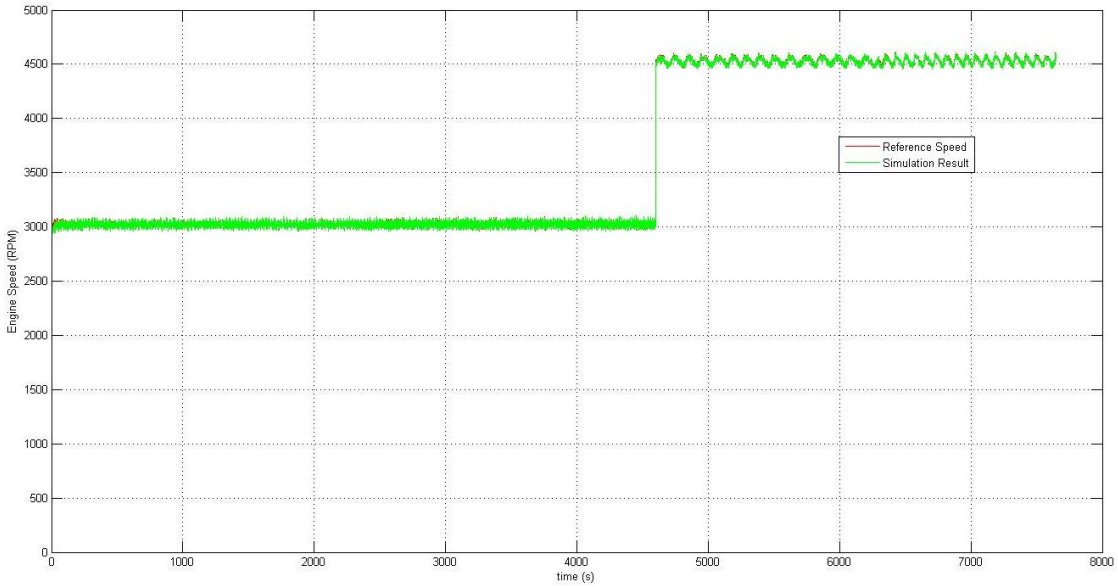

Figure 5-3. Comparison of reference generator speed and simulated generator speed when the Run 9 used

The Figure 5-4 shows the comparison of reference output power of generator and output power of the APU model when dataset Run 9 is used.

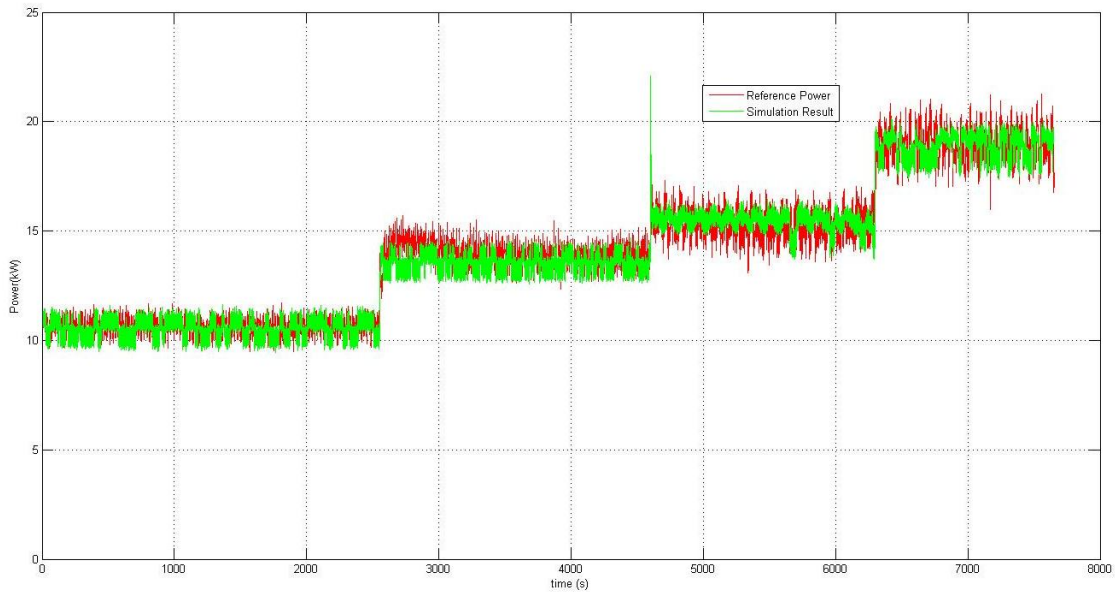

Figure 5-4. Comparison of reference output power of generator and simulated output power of generator when the Run 9 used

The Table 5-2 shows the error between the reference data and the simulation results. From the table, we can see that the APU model works very well.

			Mean	RMS
Run 4	Speed: 3500 rpm		2.0444	0.0044
	Power	Throttle: 20%	0.2078	0.8758
		Throttle: 40%	0.0264	0.6111
Run 9	Speed: 3000 rpm		1.636	0.0036
	Power	Throttle: 20%	0.1003	0.5708
		Throttle: 40%	0.4519	0.7476
	Speed: 4500 rpm			
	Power	Throttle: 20%	0.1888	0.8234
		Throttle: 40%	0.0028	0.9245

Table 5-2. Error between the reference data and the simulation results

With the engine map and efficiency map, we can get the relationship among throttle, speed and APU output power. The Figure 5-5 shows the throttle-speed-APU power map.

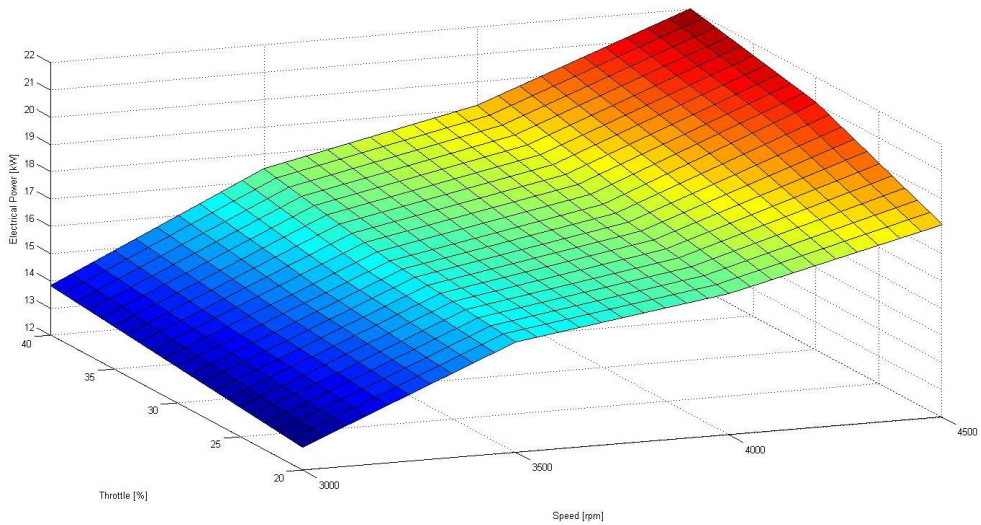

Figure 5-5. Throttle-speed-APU power map

With the engine map and BSFC map, we can get the relationship among throttle, speed and fuel consumption. The Table 5-3 and Figure 5-6 shows the throttle-speed-consumption map.

	3000rpm	3500rpm	4000rpm	4500rpm
20%	351.6 g/kWh	343.9 g/kWh	350.0 g/kWh	356.7 g/kWh
30%	348.0 g/kWh	340.3 g/kWh	345.1 g/kWh	347.1 g/kWh
40%	343.9 g/kWh	335.6 g/kWh	337.8 g/kWh	342.9 g/kWh

Table 5-3. Throttle-speed-consumption map

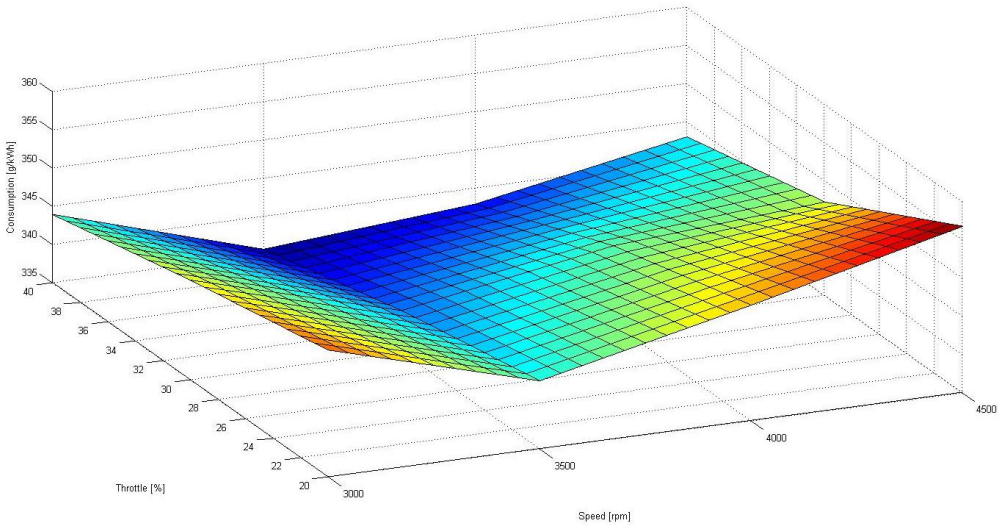

Figure 5-6. Plot of throttle-speed-consumption map

The Figure 5-7 shows the aerial views of throttle-speed-power map and throttle-speed-consumption map.

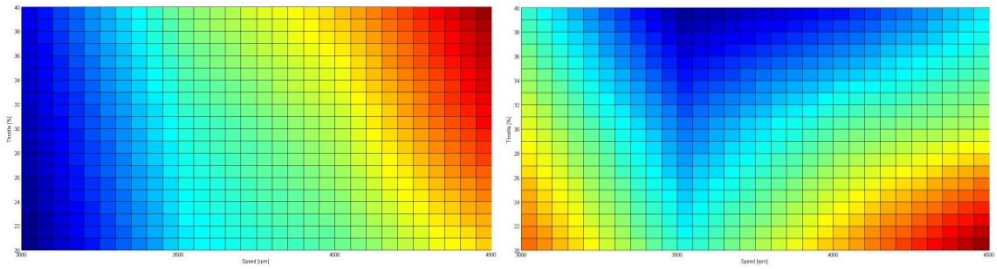

Figure 5-7. The aerial views of throttle-speed-power map (Left) and throttle-speed-consumption map (Right)

With these two maps, we can find some appropriate set points, which have less fuel consumption and appropriate power. The following table shows the three set points in this project.

Speed	Throttle	Power	Consumption
3500rpm	20%	16 kW	344 g/kWh
4000rpm	25%	17.5 kW	348 g/kWh
4500rpm	40%	22 kW	343 g/kWh

Table 5-4. The output power and fuel consumption of three set points

When the engine works at a “constant” speed, the speed actually has vibration. The Figure 5-8 shows how the vibration of engine speed looks like.

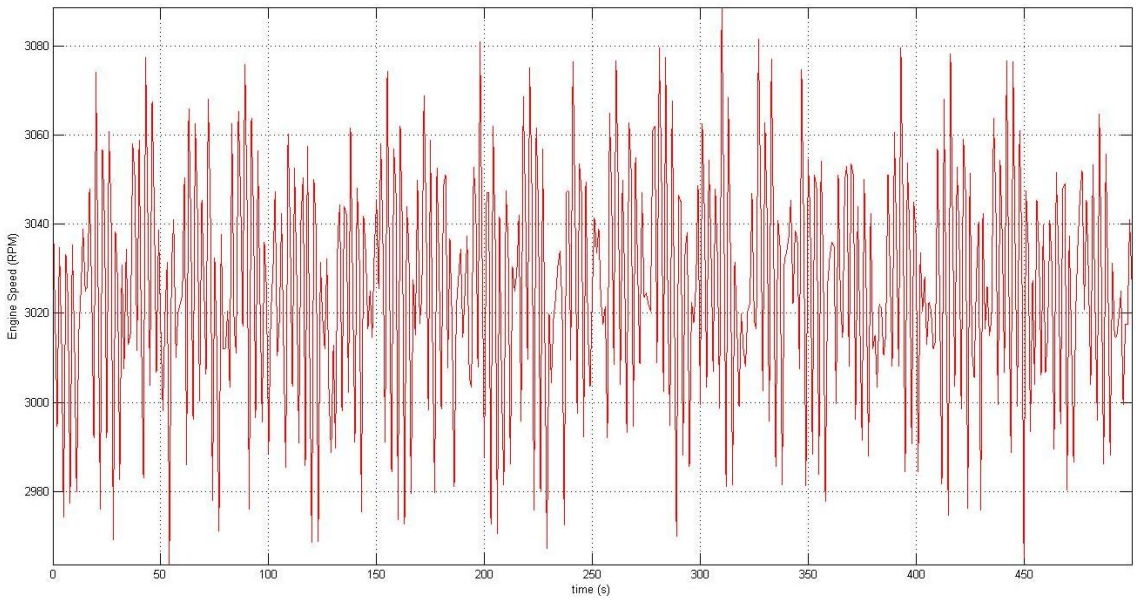

Figure 5-8. Vibration of engine speed at 3000 RPM

Ideally, when the engine works stable, the net torque should be 0, which means the total torque acting on the crankshaft equals to the load torque. In reality, however, the net torque cannot be maintained at 0 because of the torsional excitation of crankshaft and engine structure. The total torque acting on the crankshaft of the engine results from the effect of the gas and inertia forces on the crank slider mechanism [14].

The total torque is found by summing the torque resulting from piston motion, which is often called the inertia torque, and the torque resulting from gas pressure [14]. The Figure 5-9 shows the inertia torque and torque resulting from gas pressure alone for a single cylinder engine.

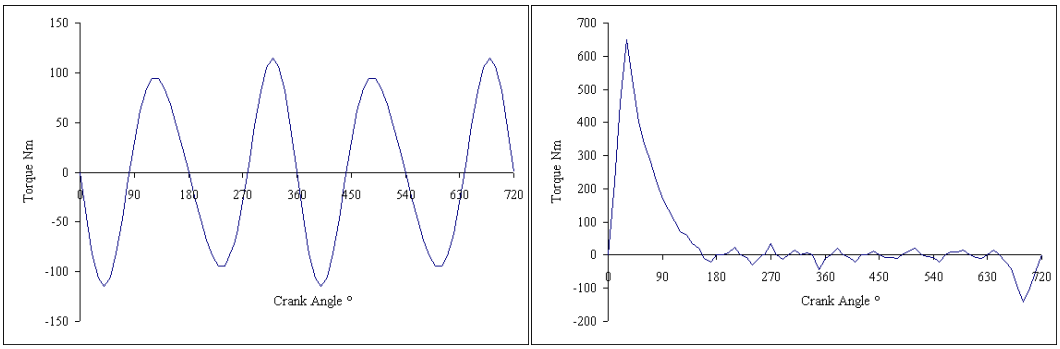

Figure 5-9. The inertia torque (Left) and torque resulting from gas pressure (Right) [14]

The Figure 5-10 shows the total torque on the crankshaft for a single cylinder engine

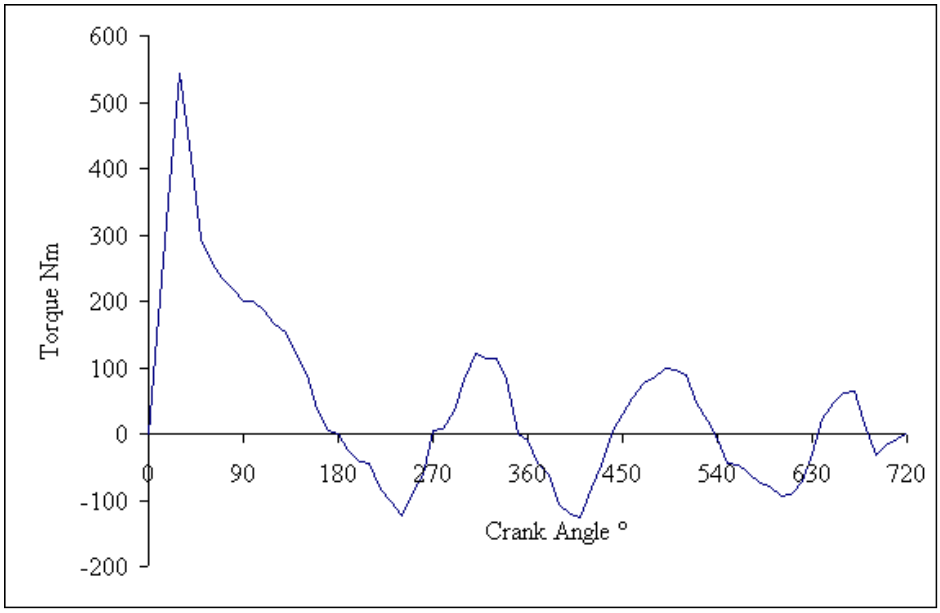

Figure 5-10. The total torque on the crankshaft for a single cylinder engine [14]

The vibration of engine speed can provide us a lot of information of the engine. Because the net torque vibration causes the vibration of engine speed, by analyzing the vibration of engine speed can give us the information of the total torque acting on the crankshaft. It can help us to control and optimize the engine work, or diagnose the working status of each cylinder of the engine.

The speed of engine/generator is controlled by generator controller. The controller of generator will use PID control loop to control the throttle position so that the generator can output stable current. Therefore, the vibration of the output current has the same frequency as the vibration of the throttle. The Figure 5-11 shows the throttle control loop.

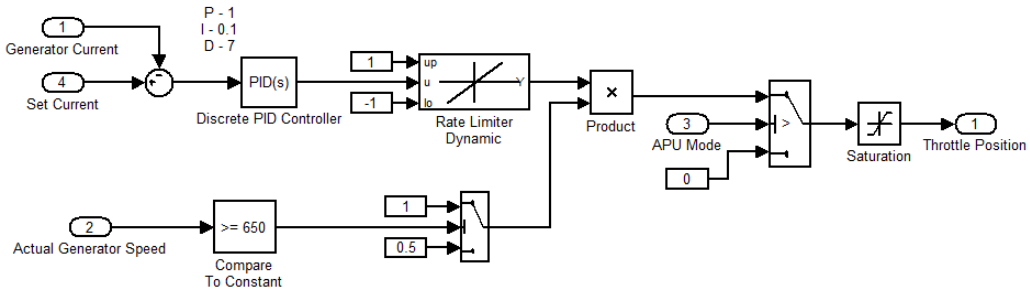

Figure 5-11. The throttle control loop

The Figure 5-12, Figure 5-13 and Figure 5-14 shows the spectra of speed vibration and current vibration.

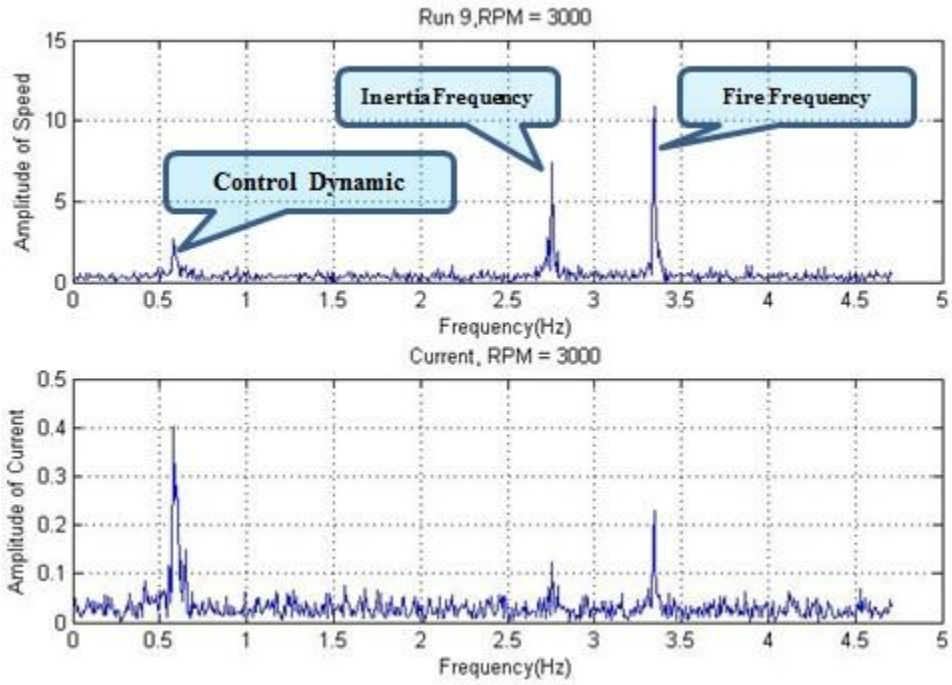

Figure 5-12. The spectra of speed vibration and current vibration at speed 3000rpm

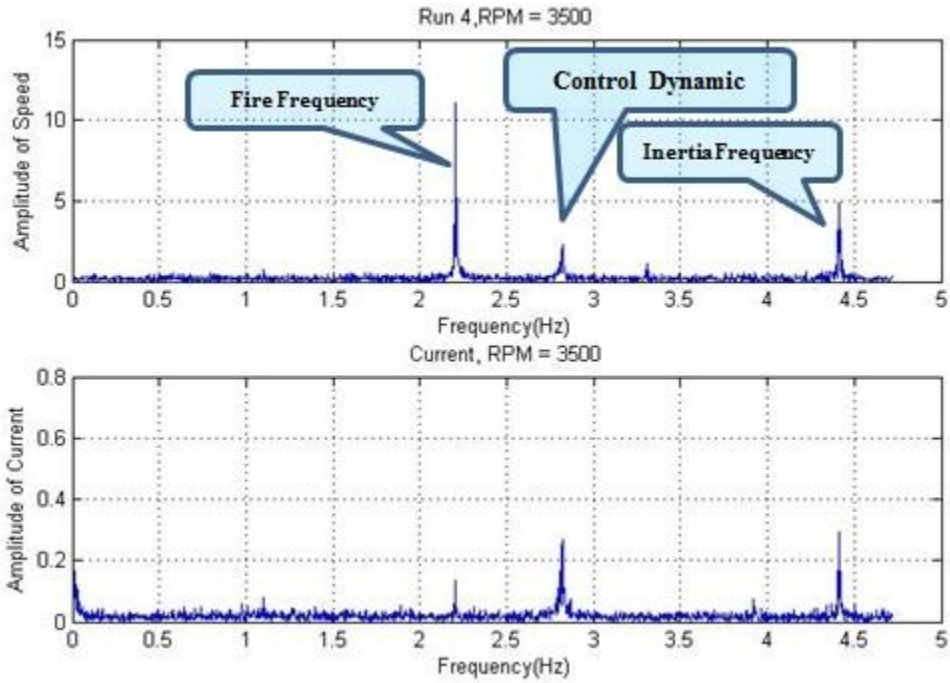

Figure 5-13. The spectra of speed vibration and current vibration at speed 3500rpm

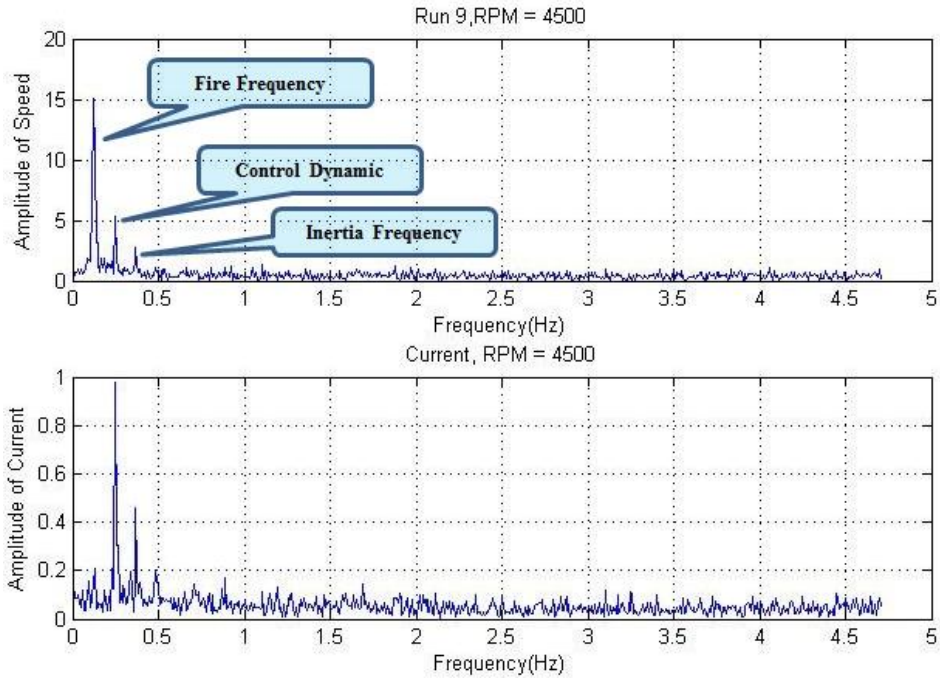

Figure 5-14. The spectra of speed vibration and current vibration at speed 4500rpm

There are three main frequencies in these figures. They are fire frequency, inertia frequency and control dynamic frequency. Because the model uses current to control the throttle and the vibration of speed is related with the vibration of the throttle, the current and the speed has the same frequency which is caused by control loop. The inertia torque and torque resulting from gas pressure will also cause the output current vibration. Therefore the fire frequency and inertia frequency also can be seen in these figures.

From these figures, we can see that when the speed is higher, the peak frequency of speed will be lower, but the amplitude of speed will be larger. Therefore we can conclude that when the speed is low, the more vibration of speed the engine has, while in the high speed state, the less vibration of speed the engine has.

The relationship between rpm and engine fire frequency is:

$$F_{fire} = \frac{\mathrm{n} \times \mathrm{rpm} \times \mathrm{i}}{120}$$

Where n is order and i is related with stroke. The Weber MPE 750 engine has 2 cylinders and 4 stroke, so n = 1 and i= 2. Therefore, the fire frequency of our engine is:

$$F_{fire} = \frac{\mathrm{rpm}}{60}$$

And the inertia frequency is $F_{inertia} = 2 \times F_{fire}$

The Table 5-5 shows the relationship among mean speed of engine, the engine fire frequency and the inertia frequency

Mean engine speed	Fire frequency	Inertia frequency
3028 rpm	50.5 Hz	101.0 Hz
3526 rpm	58.8 Hz	117.6 Hz
4523 rpm	75.4 Hz	150.8 Hz

Table 5-5. The relationship among mean speed of engine, the engine fire frequency and the inertia frequency

The sampling frequency is 9.4 Hz. The Table 5-5 shows that the sampling frequency is much lower than the fire frequency and the inertia frequency. Therefore, aliasing occurred. Aliasing is an effect that causes different signals to become indistinguishable (or aliases of one another) when sampled [1].

The frequency of the aliased signal can be represented like this:

$$F_a = \left|F_{sampling} \times n - F_{signal}\right|$$

where $F_{sampling}$ is the sampling frequency, F_{signal} is the signal frequency and n= floor($\frac{F_{signal}}{F_{sampling}} + 0.5$).

Because the sampling frequency and the signal frequency are known, the frequency of the aliased can be calculated. The Figure 5-13, 5-14, 5-15 and Table 5-6 shows the aliasing frequency.

Mean engine speed	Fire frequency	Aliasing frequency
3028 rpm	50.5 Hz	3.5 Hz
	Inertia frequency	Aliasing frequency
	101.0 Hz	2.4 Hz
Mean engine speed	Fire frequency	Aliasing frequency
3526 rpm	58.8 Hz	2.4 Hz
	Inertia frequency	Aliasing frequency
	117.6 Hz	4.6 Hz
Mean engine speed	Fire frequency	Aliasing frequency
4523 rpm	75.4 Hz	0.2Hz
	Inertia frequency	Aliasing frequency
	150.8 Hz	0.4 Hz

Table 5-6. The alias frequency

5.1.2 Simulation of APU Mode Calculation

The APU mode calculation block, which is shown in the Figure 5-15, is used to calculate the APU enable & disable status and the APU mode. All the inputs are from PSU CAN bus.

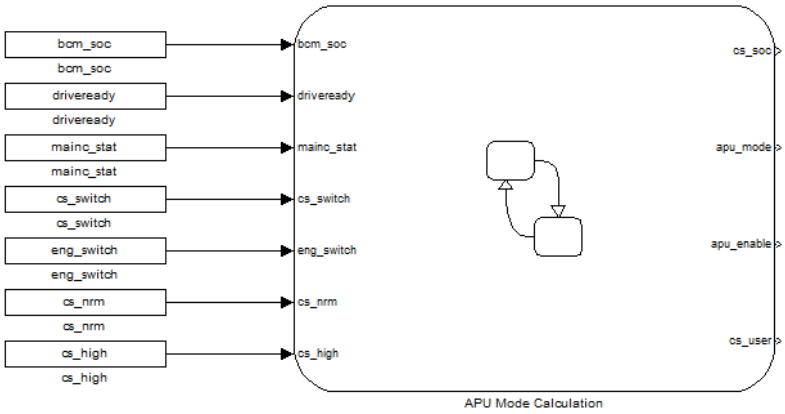

Figure 5-15. Simulation layout of APU mode calculation block

In the simulation, driveready, mainc_stat cs_nrm and cs_high are given as constant values, while the bcm_soc, cs_switch and eng_switch are variables. The Table 5-7 shows the value of these inputs.

Time	0	200	400	600	800	1000	1200	1400	1600
cs_nrm	40	40	40	40	40	40	40	40	40
bcm_soc	45	10	65	45	45	45	45	45	45
cs_switch	0-Disable	0-Disable	1-Enable	1-Enable	1-Enable	1-Enable	0-Disable	0-Disable	0-Disable
eng_switch	0-Disable	0-Disable	0-Disable	1-Enable	1-Enable	1-Enable	1-Enable	0-Disable	0-Disable

Table 5-7. The inputs of the APU mode calculation block simulation

The Figure 5-16 shows the output APU mode and APU enable & disable status of the model which simulated with the data shown in the Table 5-7.

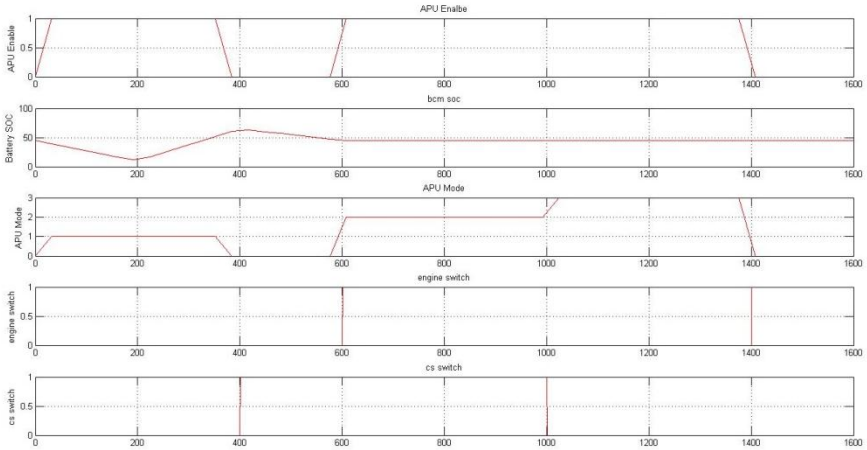

Figure 5-16. Results of the battery power calculation model simulation

The simulation results show how the battery SOC, charge sustaining switch (cs_switch) and engine switch (eng_switch) change the output APU mode. When the APU is in charge depletion mode (APU mode = 0) and the battery SOC is lower than the set point, the APU will transit to charge sustaining mode (APU mode = 1) automatically. The APU will go back from charge sustaining mode to charge depletion mode as soon as the battery SOC is higher than set point.

The engine switch and charge sustaining switch also can let the APU work in different modes. The Table 5-8 shows how these two switches affect the APU mode.

	Engine switch ON	**Engine switch OFF**
Charge sustaining switch ON	Engine charge mode APU Mode = 2	Charge susbatining mode APU Mode = 1
Charge sustaining switch OFF	Engine on mode APU Mode = 3	Charge Depletion/Charge sustaining mode APU mode = 0/1

Table 5-8. The relationship among charge sustaining switch, engine switch and APU mode

5.1.3 Simulation of Set Points Calculation

The APU mode calculation block and the set points calculation block, which are shown in the Figure 5-17, are used to calculate the throttle and engine/generator speed request.

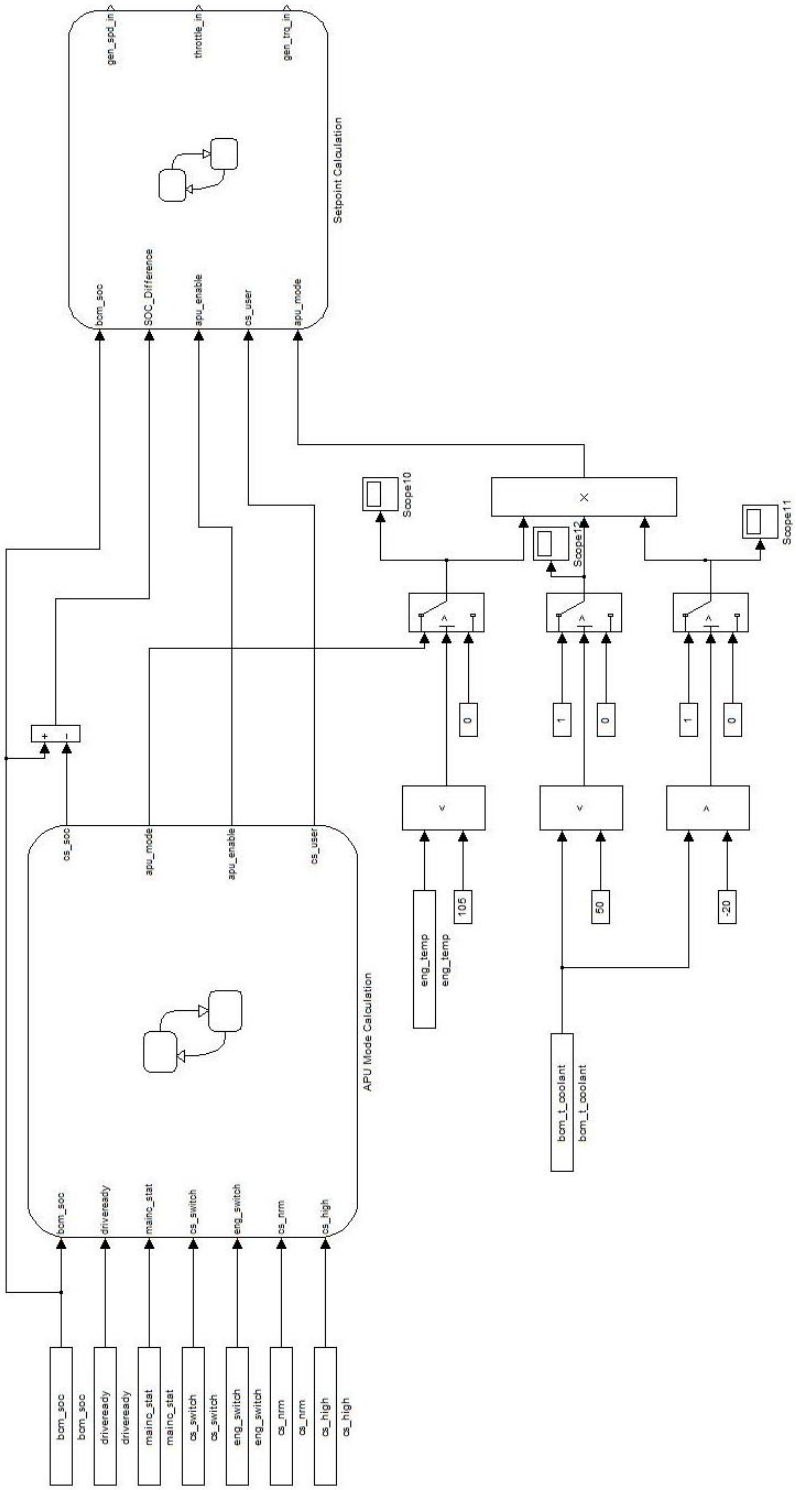

Figure 5-17. Simulation layout of APU set points calculation block

In the simulation, the inputs in Table 5-7 are used. The inputs of engine temperature and battery temperature are given to some abnormal values. The Table 5-9 shows the values of these inputs.

Time	0	200	400	600	800	1000	1200	1400	1600
cs_nrm	40	40	40	40	40	40	40	40	40
bcm_soc	45	10	65	45	45	45	45	45	45
cs_switch	0-Disable	0-Disable	1-Enable	1-Enable	1-Enable	1-Enable	0-Disable	0-Disable	0-Disable
eng_switch	0-Disable	0-Disable	0-Disable	1-Enable	1-Enable	1-Enable	1-Enable	0-Disable	0-Disable
eng_temp	80	120	80	80	80	120	120	80	85
bcm_t_coolant	30	40	60	65	45	45	-30	-10	45

Table 5-9. The inputs of the set points calculation block simulation with abnormal temperature

The Figure 5-18 shows the output throttle request and engine/generator speed request of the block which simulated with the data shown in the Table 5-9.

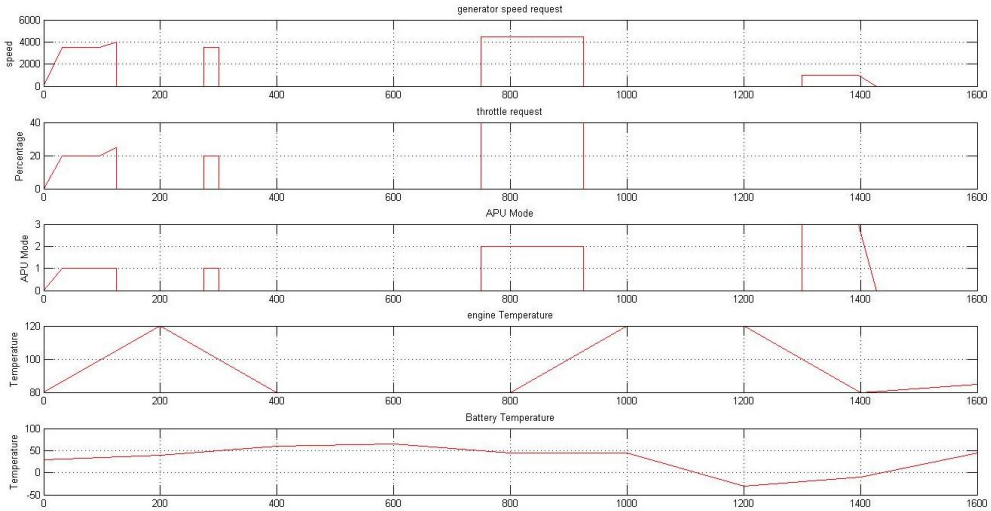

Figure 5-18. Results of the set points calculation block simulation with abnormal temperature

The Figure 5-18 shows charge sustaining switch, engine switch, battery SOC, engine temperature and battery temperature affect the set points selecting, speed request and throttle request. When the engine temperature is higher than the threshold value or

the battery temperature is higher/lower than the threshold value, the APU will be disabled and not speed request and throttle request will be outputted.

The Table 5-10 shows the values of the inputs given to the block. The engine and battery work normally.

Time	0	200	400	600	800	1000	1200	1400	1600
cs_nrm	40	40	40	40	40	40	40	40	40
bcm_soc	45	10	65	45	45	45	45	45	45
cs_switch	0-Disable	0-Disable	1-Enable	1-Enable	1-Enable	1-Enable	0-Disable	0-Disable	0-Disable
eng_switch	0-Disable	0-Disable	0-Disable	1-Enable	1-Enable	1-Enable	1-Enable	0-Disable	0-Disable
eng_temp	80	80	80	80	80	80	80	80	80
bcm_t_coolant	30	40	40	45	45	45	40	40	45

Table 5-10. The inputs of the set points calculation block simulation with normal temperature

Figure 5-19 shows the output throttle request and engine/generator speed request of the block which simulated with the data shown in the Table 5-10.

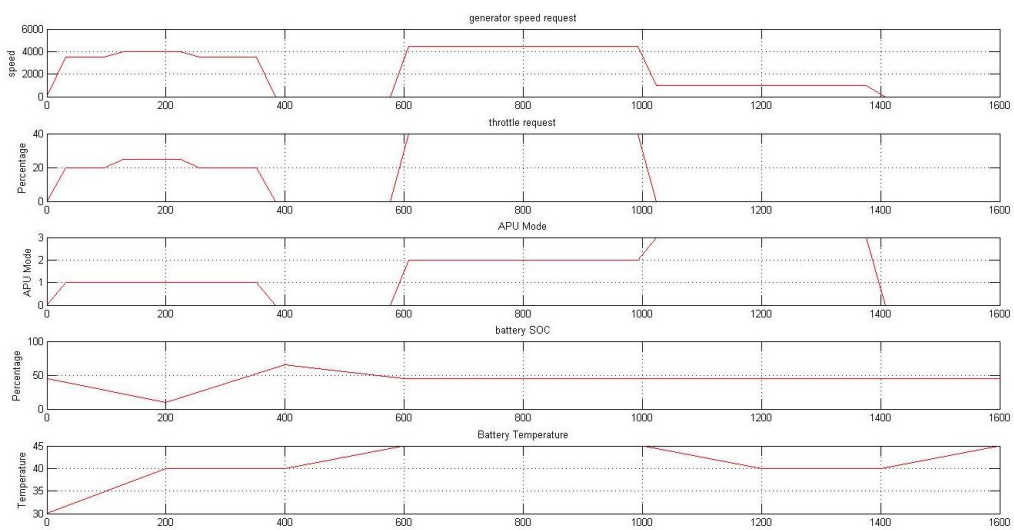

Figure 5-19. Results of the set points calculation block simulation with normal temperature

Figure 5-19 shows when the engine and battery have normal temperature, how the throttle and speed are determined. The speed request and throttle request will have different output according to different APU mode and battery SOC.

5.1.4 Simulation of Engine Control

The APU mode calculation block, the set points calculation block and the engine control block, which are shown in the Figure 5-20, are used to calculate the actual throttle and actual engine/generator speed request.

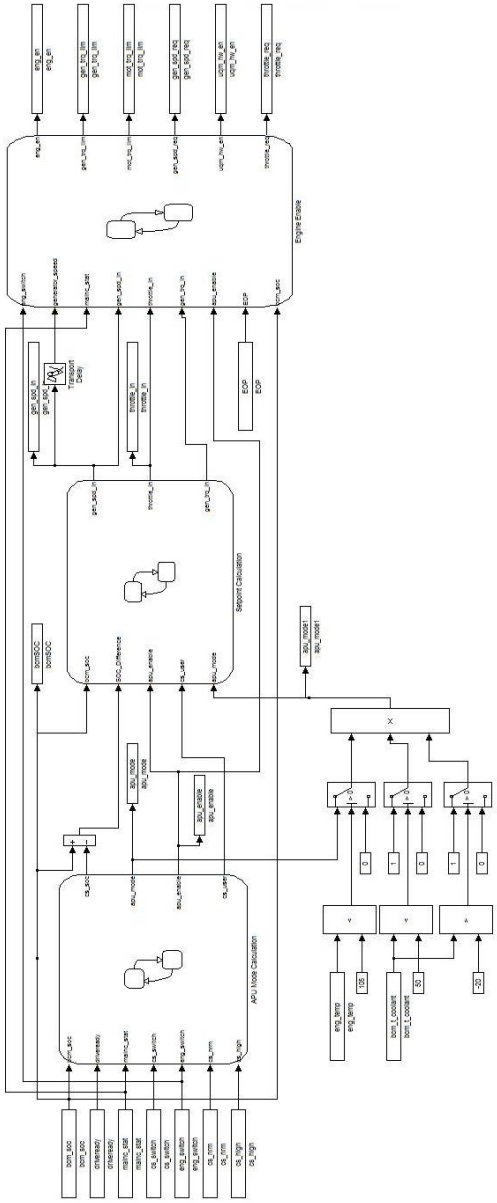

Figure 5-20. Simulation layout of engine control block

In the simulation, the inputs in Table 5-11 are used. The Table 5-11 shows the values of these inputs.

Time	0	200	400	600	800	1000	1200	1400	1600
cs_nrm	40	40	40	40	40	40	40	40	40
bcm_soc	45	10	65	45	45	45	45	45	45
cs_switch	0-Disable	0-Disable	1-Enable	1-Enable	1-Enable	1-Enable	0-Disable	0-Disable	0-Disable
eng_switch	0-Disable	0-Disable	0-Disable	1-Enable	1-Enable	1-Enable	1-Enable	0-Disable	0-Disable
eng_temp	80	80	80	80	80	80	80	80	80
bcm_t_coolant	30	40	40	45	45	45	40	40	45

Table 5-11. The inputs of the engine control block simulation

The Figure 5-21 shows the output throttle request and engine/generator speed of the block which simulated with the data shown in the Table 5-11.

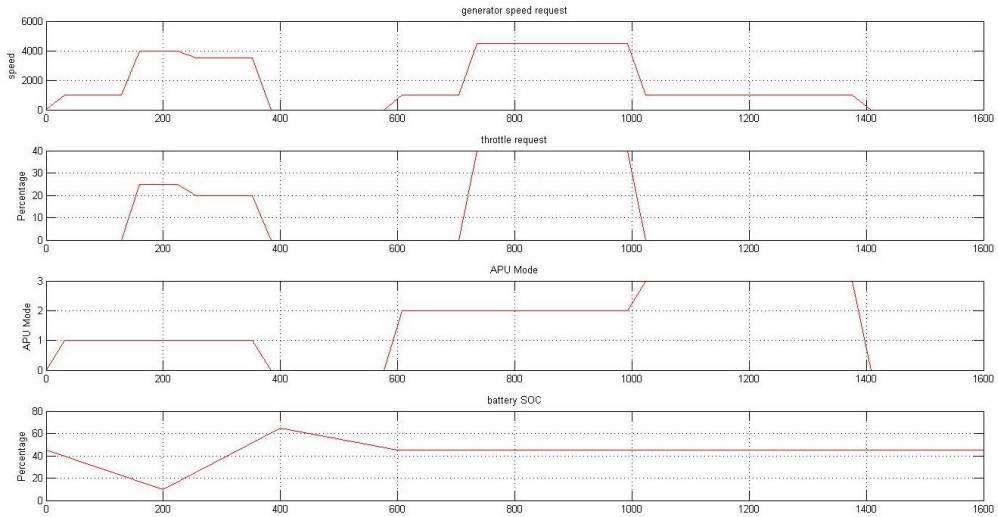

Figure 5-21. Results of the engine control block simulation

The simulation results show how the throttle and speed are finally determined. The speed of engine will be set to 1000 rpm and the engine will be given 5 seconds to crank. If the engine is successful in cranking, the speed request and throttle will be same as the output speed request and throttle request of the set points calculation function block. Otherwise, the engine will try to startup again. The throttle request and speed request will be sent to the CAN bus.

5.2 Experiment of the Auxiliary Power Unit

Two different ways of validation are used to validate the APU model and APU control algorithm.

- For APU model, data is obtained from the CAN bus. The data contains engine/generator speed, throttle and APU output power. Totally 12 points are validated.
- For APU control algorithm, the algorithm will be downloaded to the main controller. The inputs of the algorithm are from CAN bus.

5.2.1 Equipment Used

Below follows a summary of the equipment used in the experiments:

- Personal Computer, for logging data and send data to the controller via CAN bus. The program “MotoTune” runs in the computer.
- CAN bus data acquisition card, CANcaseXL Log card, is used for connecting the computer usb port to the CAN bus and collecting/sending data to the controller.
- Battery information acquisition card, for collecting information of the battery pack.

5.2.2 Measurement

The point-by-point measurement of APU model was performed with the engine and throttle running at different speed, and the output power of APU was recorded. The MotoTune program was used to send data to CAN bus and collect data from CAN bus. The Figure 5-22 shows how each point is measured.

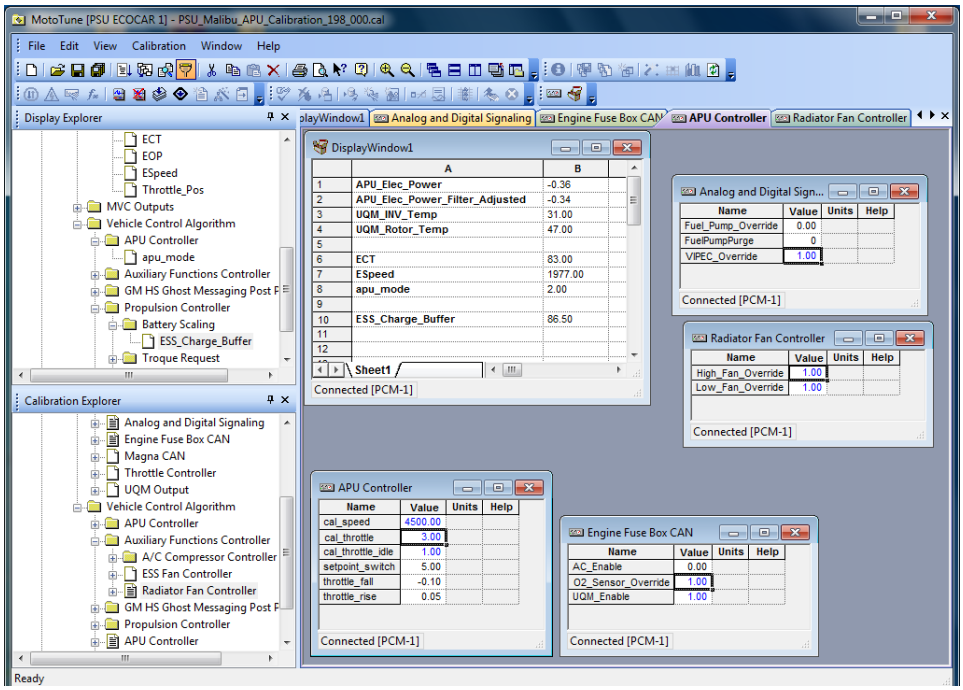

Figure 5-22. Measurement of APU model

The speed value was written into the “cal_speed” row and the throttle value was written into the “cal_throttle” row. Then the APU output power could be observed in the “APU_Elec_Power” row.

The Table 5-12 shows all the data got from point-by-point measurement.

	3000rpm	3500rpm	4000rpm	4500rpm
20% Throttle	12 kW	15.5 kW	18 kW	20 kW
30% Throttle	13 kW	17 kW	19 kW	21 kW
40% Throttle	13.5 kW	17.5 kW	20 kW	22 kW

Table 5-12. Result of point-by-point measurement

The experiment of APU control algorithm was performed with different charge sustaining switch status, engine switch status and battery SOC, and the output APU mode, generator speed request and throttle request are shown in the MotoTune program. The Figure 5-23 shows how these data were collected and validated.

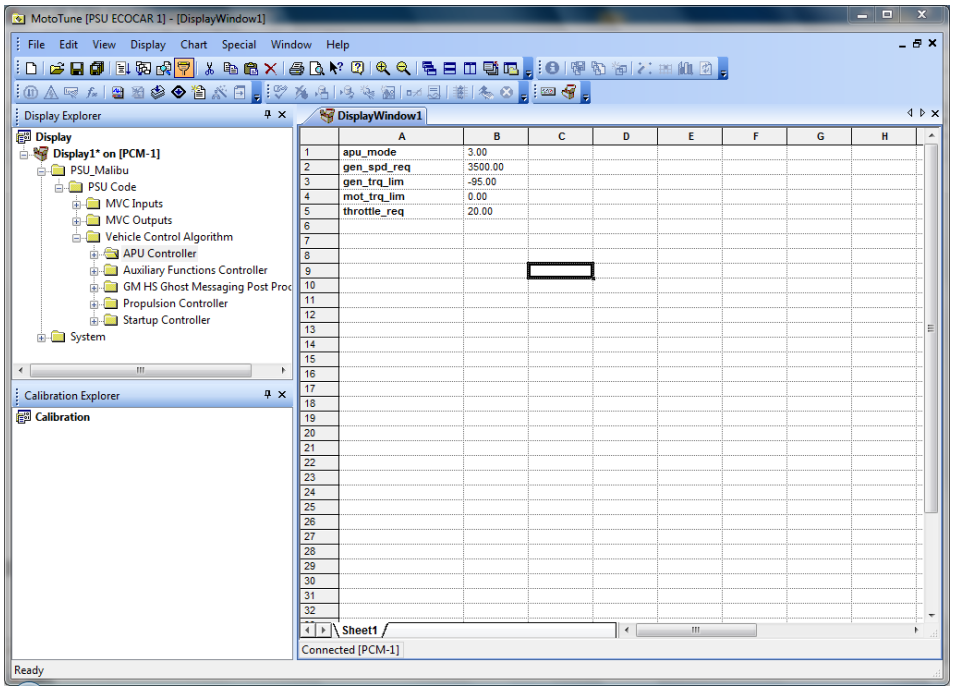

Figure 5-23. Measurement of APU control algorithm

5.2.3 Results

The main effort in the project was to develop the APU model and the APU control algorithm, and use them to estimate the output power and the fuel consumption.

The Table 5-13 shows the comparison between measured APU output power and the result of APU model simulation.

		3000rpm	3500rpm	4000rpm	4500rpm
20% Throttle	Measured data	12 kW	15.5 kW	18 kW	20 kW
	Output of APU model	12.8 kW	16 kW	17.2 kW	19 kW
30% Throttle	Measured data	13 kW	17 kW	19 kW	21 kW
	Output of APU model	13.3 kW	16.5 kW	18 kW	21 kW
40% Throttle	Measured data	13.5 kW	17.5 kW	20 kW	22 kW
	Output of APU model	13.8 kW	17.4 kW	19.2 kW	22 kW

Table 5-13. Result of point-by-point measurement and result of APU model simulation

This table shows that the result of APU model simulation is very close to the real output power of APU. Therefore, with this APU model, we can use the model to calculate the output power of APU, engine torque and fuel consumption.

The APU control algorithm can enable/disable the APU and/or determine the engine/generator speed request and throttle request. The experiment shows the algorithm can output appropriate speed request and throttle request according to battery SOC, charge sustaining switch and engine switch status.

Chapter 6

Summary and Conclusions

6.1 Summary

The aim of this study is to develop a computer model and control strategy for the Auxiliary Power Unit (APU) of a series Plug-in Hybrid Electric Vehicle built by the Penn State Advanced Vehicle Team for the EcoCAR 2 competition.

The APU model has been developed using MATLAB/SIMULINK. It includes three lookup tables: engine torque map, engine brake specific fuel consumption map, and generator efficiency map. These maps were developed from manufacturer supplied data and test data. They were refined using various interpolation methods. Without the need to have the complex measurement, the APU model simulation also gave fuel economy estimations. The PI control loop of the APU model has been tuned, so the model can find the appropriate generator torque and output engine speed according to the speed command.

The spectrum of the measured engine speed has been analyzed and compared to the spectrum of the output current of the generator. It shows how the control dynamic of the generator, air pressure torque and inertia torque effect the speed dynamic of the engine speed.

With the APU model developed and tuned, the focus then shifted to developing and validating the APU control algorithm. The control algorithm was developed and simulated in Simulink and then it was downloaded into the controller of the vehicle and

tuned. The control algorithm can send appropriate command and parameter to the APU according to the different condition.

6.2 Future work

The engine dynamic control is an important consideration. This thesis analyzed the spectrum of the measured speed and the current. High frequency vibration of engine speed will cause more unpredictable fuel consumption. Therefore, it is important to build the throttle model and control algorithm to reduce the frequency of vibration of the engine speed.

The control algorithm developed for this thesis can continue to be refined. Presently, the APU is only run at three set points. It is not an economical way to use the APU. The APU power request mode could be designed and added so that the engine operating range can be further opened. Another area that can be improved is the performance of the engine. The design of the current APU control algorithm is optimized the power of the APU. The fuel consumption does not have much weight in the algorithm. The performance of the engine could be more optimized so that the performance of APU could be more balanced.

Appendix

Vehicle Model

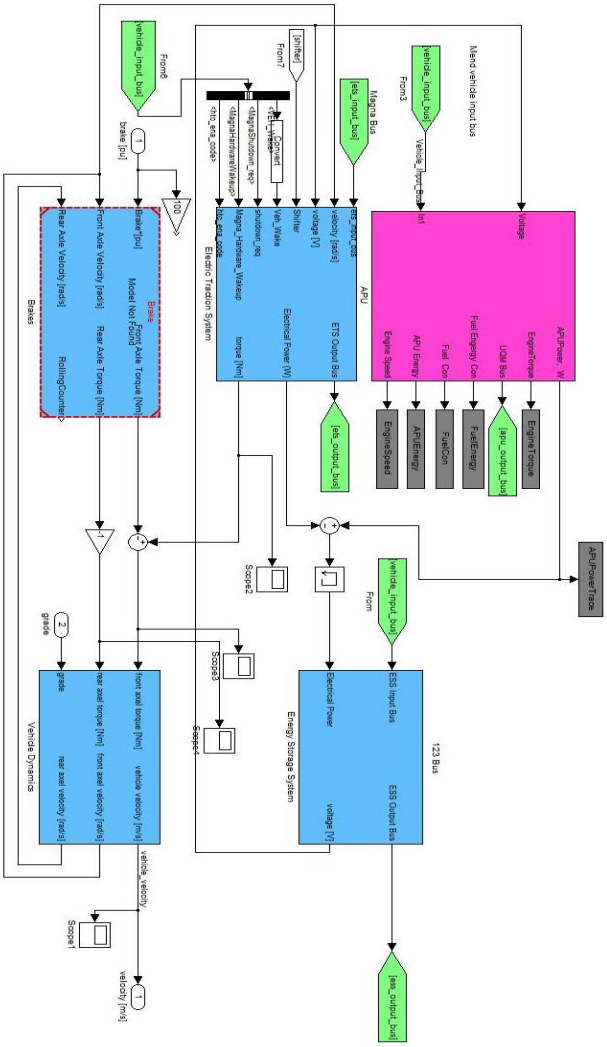

References

1. Wikipedia, http://en.wikipedia.org/wiki.
2. U.S. Energy Information Administration, http://www.eia.gov/.
3. Carbon Dioxide Information Analysis Center, http://cdiac.ornl.gov.
4. Yuliang Leon Zhou, "Modeling and Simulation of Hybrid Electric Vehicles", Master's Thesis, University of Victoria, 2007.
5. Brad Berman, "History of Hybrid Vehicles", http://www.hybridcars.com/history-of-hybrid-vehicles, 2011.
6. Gavin M. Cotter, "A study in Hybrid Vehicle Architectures: Comparing Efficiency and Performance", Bachelor's Thesis, Massachusetts Institute of Technology. http://mit.dspace.org/bitstream/handle/1721.1/54531/565894813.pdf?sequence=1, 2009.
7. Sergio Grammatico and Andrea Balluchi, "A series-parallel hybrid electric powertrain for industrial vehicles", Vehicle Power and Propulsion Conference 2010.
8. EcoCar 2, http://www.ecocar2.org/.
9. Daniel Haworth, Jeffrey Mayer, Gary Neal, "Implementation and Validation of a Series Plug-In Hybrid Electric Vehicle", Final Technical Report for Penn State AVT Entry in EcoCAR 2, 2013.
10. Weber MPE 750 manual, Weber Motor GmbH, http://www.weber-motor.com.
11. PowerPhase® 75 Traction System manual, UQM Technologies Inc., http://www.et.aau.dk/digitalAssets/46/46824_uqm_powerphase_75.pdf .
12. Steve Corrigan, "Introduction to the Controller Area Network (CAN)", Application Report of Texas Instruments, 2008.

13. Wonhee Lee, “Computer Simulation of a Series and Parallel Hybrid Electric Vehicle”, Master’s Thesis, Durham University, 1999.
14. Paul Hollingworth, “Engine Excitation Mechanisms”, Science and Engineering Encyclopedia, http://DiracDelta.co.uk.
15. Andrew W. Spiegel, “Method for Reducing Engine Cold Start Emissions from Transient Fueling in an Alternative Fueled Engine”, Undergraduate Honors Thesis, The Ohio State University, 2013.
16. Petter Strandh, “Combustion Engine Models for Hybrid Vehicle System Development”, Project Report, Lund Institute of Technology, 2002.
17. Qing Wang, et. al., “Vehicle System Controls for a Series Hybrid Powertrain”, SAE technical paper 2011-01-0860, 2011.
18. Eric John Schacht, “Design and Development of the EcoCAR Vehicle and the Vehicle Controls Providing Efficiency and Drivability”, Master’s Thesis, The Ohio State University, 2011.
19. J. Marco and E. Cacciatori, “The Use of Model Based Design Techniques in the Design of Hybrid Electric Vehicles”, 3rd Institution of Engineering and Technology Conference Automotive Electronics, 2007.
20. Saurabh Mahapatra and Tom Egel, “Model-Based Design for Hybrid Electric Vehicle Systems”, SAE technical paper 2008-01-0085, 2008.